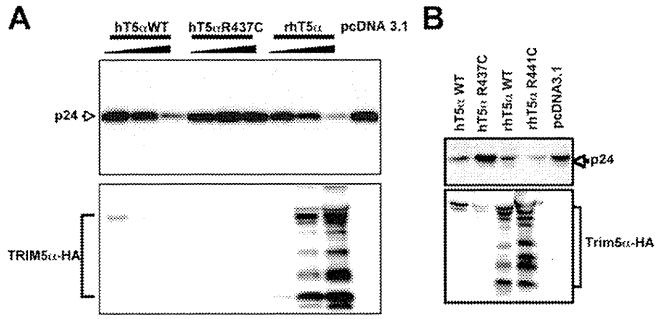

Fig. 2. Incorporation of TRIM5α into HIV-1 virion. Culture supernatants of the 293T cells co-transfected with pNLΔpolEGFP and various TRIM5α plasmids were harvested and passed through 0.45 μm filter followed by ultracentrifugation through 20% sucrose layer. The VLP fractions prepared from 1 ml out of total 2 ml culture medium were applied to immunoblotting to detect the HIV-1 Gag proteins and incorporated TRIM5α. (A) pNLΔpolEGFP (0.01 μg) was transfected together with increasing amounts of TRIM5α_{hu}-HA (hT5αWT or R437C) and TRIM5α_{rh}-HA expression plasmid (rhT5α) as indicated in Fig. 1B. (B) pNLΔpolEGFP (0.01 μg) was transfected along with 0.1 μg of TRIM5α_{hu}-HA (hT5αWT or R437C) or 0.05 μg TRIM5α_{rh}-HA expression plasmid (rhT5αWT or R441C).

readily detected in VLP lysates and was inversely correlated with P24 levels, less amount of wild type TRIM5α_{hu} was detected in VLP fractions, and the mutant TRIM5$_{hu}$ was only marginally existent or even absent (Fig. 2A). These results suggest TRIM5α_{hu} has weaker affinity for Gag than TRIM5α_{rh}, which is consistent with our finding that TRIM5α_{rh} inhibited HIV-1 more strongly than wild type TRIM5α_{hu} (Fig. 1B).

3.3. The corresponding mutation in TRIM5α_{rh} has no effect on its late restriction activity

An important question is that whether this arginine is also required for rhesus TRIM5α, since it had been reported that SPRY domain of TRIM5α_{rh} is dispensable to inhibit HIV-1 production [17,21]. We mutated arginine residue to cysteine at 441a.a. of TRIM5α_{rh}, which corresponds 437a.a. of TRIM5α_{hu}, and selected a clone that can express the HA-tagged mutant TRIM5α_{rh} protein at the same level as the wild type. We co-transfected the TRIM5α_{rh} mutant with pNLΔpolEGFP to 293T cells, and then investigated the effect of the mutant on HIV-1 production and encapsidation into virions. As shown in Fig. 2B, R441C TRIM5α_{rh} mutant restricted HIV-1 production as severely as the wild type, and similar amounts of both wild type and mutant TRIM5α_{rh} proteins were incorporated into virions. These results are in consistence with Sakuma's report [17,21].

3.4. Knockdown of endogenous TRIM5α restores HIV-1 production

To examine the inhibitory effect of TRIM5α_{hu} under physiological conditions, siRNA was used to suppress TRIM5α_{hu} expression. Human HT1080 or 293T cells were co-transfected with pNLΔpolEGFP and control siRNA or siRNA against TRIM5α_{hu}. As shown in Fig. 3A, p24 production was enhanced roughly 3 fold upon knockdown of TRIM5α_{hu} in HT1080 cells but was not altered in 293T cells in which TRIM5α_{hu} was expressed at low levels. In parallel, the amount of cellular TRIM5α_{hu} mRNA was markedly reduced in HT1080 cells, but much less in 293T cells (Fig. 3A left panel). It was noted that 293T cells produced over 170 times more p24 (58.68 ng/ml and 0.34 ng/ml, respectively) and expressed 110 times higher β-galactosidase activities (data not shown) than HT1080 cells, probably because of the better efficiency of transfection to 293T cells.

Next, we examined the effect of TRIM5α_{hu} knockdown on HIV-1 production in HIV-1 host cells. As a first step, we examined the level of expression of TRIM5α_{hu} in several T and macrophage cell lines (such as Jurkat, Molt4, MT-4, U937, and HL60) by quantitative RT-PCR and found that Jurkat E6-1 cells express the highest level of TRIM5α_{hu} mRNA (Supplemental Information Fig. 1). We then transfected pNLΔpolEGFP to these T cell lines by electroporation and evaluated the p24 production in the culture media. While JurkatE6-1, Molt4, and MT-4 showed similar transfection efficiency, MT-4 produced highest level of p24 (2.34 ng/ml) compared with Molt4 and JurkatE6-1 (250 pg/ml and 114 pg/ml, respectively). This is reverse relation to the levels of Trim5α_{hu} mRNA (Supplemental Information Fig. 2). Next we examined the effect of TRIM5α knockdown on HIV-1 production in JurkatE6-1 cells. siRNA against TRIM5α_{hu} together with pNLΔpolEGFP were electroporated into the cells. Forty-eight hours later, the abundance of TRIM5α_{hu} mRNA was reduced to 35%, and concomitantly the amount of p24 Gag in the culture media was increased about 2.5 times compared to control siRNA (Fig. 3B). These results demonstrate that endogenous TRIM5α_{hu} is able to restrict HIV-1 progeny production.

3.5. Effect of the TRIM5α_{hu} R437C mutant on HIV-1 entry

The mutation R437C in TRIM5α_{hu} is located in the SPRY domain, in which alteration of a single amino acid has been reported to modulate TRIM5α restriction potency against HIV-1 infection at an early stage [35]. Therefore, we examined whether there was any difference between wild type TRIM5α_{hu} and the R437C mutant in restricting HIV-1 infection early in infection. At first we examined the effects of various Trim5αs, which were transiently expressed in 293T cells by transfection of pHuT5αWT, pRhT5α, and pHuT5αR437C, on the efficiency of infection of HIV-1-Venus that had been pseudotyped with VSV-G glycoprotein. The cells expressing TRIM5α_{hu}WT and TRIM5α_{hu} R437C showed slightly decreased rate of HIV-1-Venus infection compared with the control vector pcDNA3.1-transfected cells, whereas TRIM5α_{rh}-expressing cells were markedly resistant (Fig. 4A). To confirm this result, using a retrovirus vector we established stable HeLa cells that express TRIM5α_{hu}WT, TRIM5α_{hu} R437C, and TRIM5α_{agm}The cells were then infected with pesudotyped HIV-1-Venus as above. Similarly, TRIM5α_{agm}-

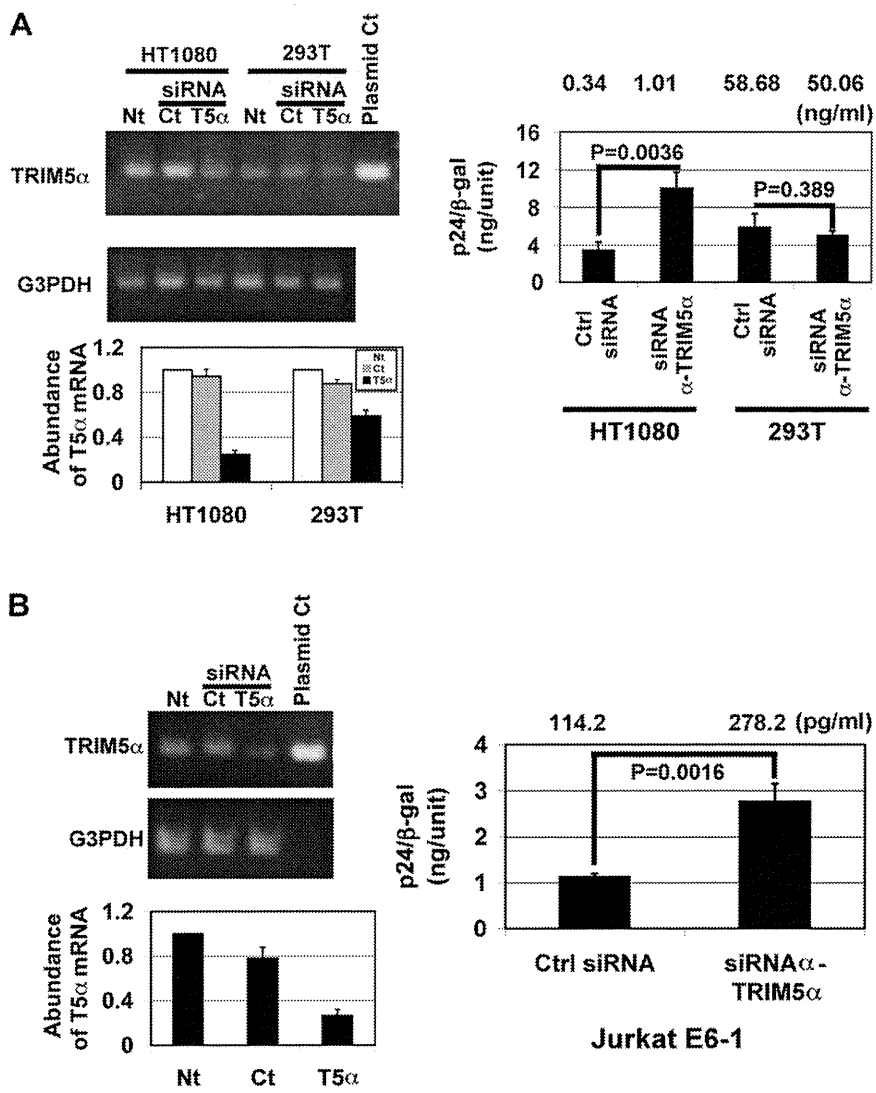

Fig. 3. Effect of knockdown of TRIM5α in human cells on HIV-1 production. (A) HT1080 or 293T cells were co-transfected with pNLΔpolEGFP and control siRNA or siRNA against Trim5α_{hu}. (B) Jurkat E6-1 cells were electroporated with the plasmid and siRNAs described above by nucleofection. pCDM-β-gal was also included in both A and B to monitor the transfection efficiency. After 2 days, p24 levels in the supernatants and β-gal activity in the cell lysates were measured. The relative p24 production was calculated by dividing p24 amount by β-gal activity (right panel of A and B). The p24 levels in the culture media are indicated on the top of right panels of A and B. The level of TRIM5α expression was examined by usual and quantitative RT-PCR. Cells that were not subjected to any treatment (Nt) were used as blank controls. The pictures of RT-PCR in the left panels represent a typical one of 3 independent experiments. The results of quantitative PCR represent the mean ± S.D. of triplicate samples.

expressing cells were markedly resistant to infection, By contrast, the marginal inhibitory effect on HIV-1 infection was observed for the cells expressing TRIM5α_{hu}WT and TRIM5α_{hu} R437C (Fig. 4C). Since all TRIM5αs were identically expressed (Fig. 4B and D), the difference in HIV-1 infection efficiency was not due to differences in TRIM5α levels. These results suggest that the mutation at residue 437 of TRIM5α_{hu} has subtle effect on HIV-1 infection at the post-entry stage.

3.6. Effect of TRIM5α_{hu} R437C on N- and B-MLV infection

TRIM5α_{hu} has been shown to restrict N-tropic but not B-tropic MLV infection [10]. Since the coiled-coil and the SPRY domains have been reported to be involved in this processes, we investigated whether the amino acid substitution at residue 437 in the SPRY domain alters the ability of TRIM5α_{hu} to inhibit N-tropic MLV infection. Wild type and mutant TRIM5α expressing 293T cells were established and infected with VSV-G-pseudotyped N-tropic and B-tropic MLV at various doses. In comparison with 293T cells transduced with the empty MX-puro vector, cells expressing wild type TRIM5α_{hu} or TRIM5α_{agm} were markedly resistant to infection with N-MLV but susceptible to B-tropic MLV, consistent with previous reports [36] (Fig. 5A). N-tropic MLV was infected to the R437C mutant expressing cells as efficiently as cells transduced with the empty MX-puro vector. Cells expressing TRIM5α_{rh} were susceptible as well,

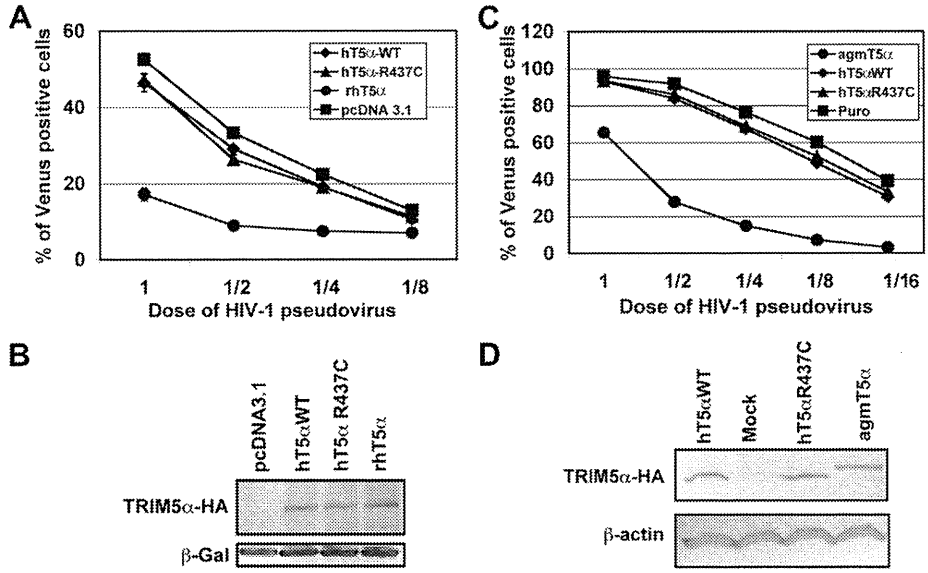

Fig. 4. Effect of various TRIM5αs on HIV-1 entry. 293T cells were transfected with TRIM5α_{hu}-HA (hT5αWT or R437C) or TRIM5α_{rh}-HA (rhT5α) expression plasmid, and then infected with VSV-G pseudotyped HIV-1-Venus (A). HeLa cells that had been transduced with various TRIM5α encoding retrovectors were infected with VSV-G pseudotyped HIV-1-Venus (C). Forty-eight hours after infection, the cells were harvested and the Venus-positive cells were counted by FACS. (A and C)shows a typical result of three independent experiments. (B and D) The expression of TRIM5α was examined by immunoblot assay.

which is consistent with the published data [37]. These results indicate that the amino acid 437 in the SPRY domain is involved in the ability of TRIM5α_{hu} to suppress both HIV-1 production and N-MLV infection.

4. Discussion

Sakuma et al. reported an inhibitory effect of TRIM5α_{rh} at a late phase of HIV-1 replication [17]. In this study we extended this finding to TRIM5α_{hu} and showed that this effect is specific, using a loss of function point mutant (TRIM5α_{hu}R437C). Although TRIM5α_{hu} has weaker ability to block the HIV-1 production than TRIM5α_{rh}, the knockdown experiment clearly showed that endogenous TRIM5α_{hu} do inhibit the HIV-1 production. The ability of TRIM5α_{hu} to reduce the production of HIV-1 some extent has also been reported previously [Supplementary Fig. 2 of 17,18]. Accordingly our results suggest that endogenous TRIM5α_{hu} functions as an innate immunity molecule that reduces HIV-1 production.

The RING, B-box2 and coiled-coil motifs (RBCC) of TRIM5α_{rh} have been reported to be essential for blocking

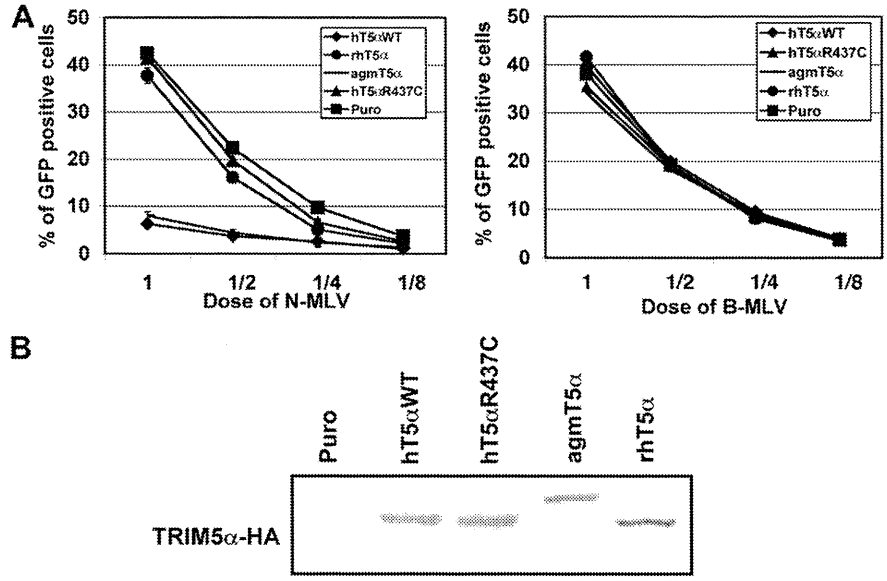

Fig. 5. Effect of various TRIM5αs on N-MLV infection. The 293T cells transduced with various TRIM5α encoding retrovectors were infected with VSV-G-pseudotyped GFP encoding N and B-tropic MLVs. Forty-eight hours after infection, the cells were harvested and GFP-positive cells were counted by FACS. (A) The left panel includes the means ± S.D, which was calculated based on three independent experiments. The right panel represents a typical result of 2 independent experiments. (B) The expression of TRIM5αs was examined by immunoblot assay.

HIV-1 production. Particularly RING and B-box domains have been identified to regulate the interaction between TRIM5α_{rh} and HIV-1 Gag, while the coiled-coil domain determines the late restriction activity [21]. Our results suggest that the SPRY domain of TRIM5α_{hu} is also involved in this restriction and that arginine at reside 437 is important, since the arginine to cysteine mutation severely abolished HIV-1 inhibition (Fig. 1B and C). However, its importance is limited to TRIM5α_{hu}, as introduction of corresponding mutation into TRIM5α_{rh} did not alter the restriction activity of TRIM5α_{rh}. TRIM5α_{hu} specific effect of the Arg to Cys mutation is concordant with the reduction of affinity between TRIM5α and Gag, which was demonstrated by the encapsidation of TRIM5α into VLP. Since the affinity of TRIM5α_{hu} to Gag was naturally weaker than that of TRIM5α_{rh}, the effect of the mutation in TRIM5α_{hu}, but not TRIM5α_{rh}, may become phenotypically apparent.

The critical motif on the restriction at early stage of retroviral infection has been reported to lie between residues 332–340 of TRIM5α_{hu}, which shows the greatest sequence diversity among human, rhesus and African green monkey TRIM5αs [36,38,39]. For example, a single amino acid substitution (R332P) conferred the ability to restrict HIV-1 to TRIM5α_{hu} [39,40]. A change of tyrosine 336 to alanine or lysine TRIM5α_{hu} enabled restriction of B-MLV, NB-tropic Moloney MLV and SIVmac [41,42]. The arginine at residue 437 of TRIM5α_{hu} is located outside the motif and conserved among human, rhesus and rodent Trim5s (accession numbers: NM_001014023.1, NM_175677.4, and NP_001014045). Therefore, our results reveal that the C-terminal conserved region of the SPRY domain is also involved in the interaction of TRIM5α to HIV-1 Gag so as to play an important role in restriction of both HIV-1 production and human resistance to MLV infection. Since rodents are susceptible to MLV infection, the other portion besides Arg437a.a. of TRIM5α_{hu} should be also involved in the restriction effect on N-MLV infection.

Although Sakuma et al. reported that overexpression of TRIM5α_{rh} reduced both HIV-1 p55 and p24 levels, we observed reduction only of p24, while p55 levels remained constant (Fig. 1C). Instead, we noted TRIM5α_{hu} dependent reduction of p38, a processing intermediate of the HIV-1 Gag protein. This difference may be ascribed to more efficient Gag processing in our system, or insensitive detection of p55 by the anti Gag monoclonal antibody [34] used in this study. These results are not inconsistent with the proposed hypothesis that TRIM5α reduces HIV-1 production by degradation of HIV-1 Gag polyproteins. However, we cannot rule out the possibility that TRIM5α_{hu} may inhibit HIV-1 production by a different mechanism, because only low incorporation of TRIM5α_{hu} was observed in HIV-1 VLPs in contrast to the abundant incorporation of TRIM5α_{rh}. TRIM5α_{hu} might be involved in the HIV-1 Gag maturation rather than degradation of the polyproteins.

Although HIV-1 is known to replicate well in human cells, HIV-1 infection generally progresses to a latent stage that shows few or no symptoms and that can persist for decades. Adaptive immune responses such as those mediated by cytotoxic T cells (CTL) and the humoral system suppress viral replication during chronic infection. Aspects of the innate immune system can also contribute to viral suppression during chronic infection. For example, Apobec3G is induced in macrophages by IFN-α and reduces HIV-1 production even if the virus expresses the anti-Apobec3G factor Vif [9]. The ability of TRIM5α_{hu} to restrict HIV-1 production suggests that it may also constitute an innate immunity factor that functions to lower virus replication levels and elicit a long nonsymptom phase.

A considerable number of polymorphisms in TRIM5α_{hu} have been documented. Although the majority of them are not associated with susceptibility to HIV-1 infection [43–45], one common nonsynonymous single nucleotide polymorphism (SNP), R136Q, affects acquisition of HIV-1 infection [45]. A recent report by Torimiro et al. [46] revealed that about 4% of Baka pygmies in Cameroon were heterozygous for a truncation mutant of TRIM5α (R332X), which completely loses the ability to restrict HIV-1 infection. The Trim5α_{hu}R437C mutant in our study was amplified from the cDNA from peripheral blood mononuclear cells of an individual, suggesting the existence of another SNP related to retrovirus infection susceptibility although it cannot be ruled out that the mutation was introduced during PCR.

Taken together, our data provides evidence that endogenous human TRIM5α possesses suppressive activity at the step of HIV-1 progeny production, supporting the hypothesis that it comprises part of the innate immune system that limits HIV-1 replication. This notion is in line with data showing IFN-α treatment increases the levels of TRIM5α_{hu} mRNA and enhances antiviral activity against N-MLV infection [47]. IFN-α treatment also up-regulates TRIM5α mRNA in rhesus monkey cells, which correlates with enhanced TRIM5α-mediated pre- and post-integration restriction of HIV-1 replication [8]. Further investigation of the mechanisms by which TRIM5α_{hu} prevents production of HIV-1 may provide valuable information for antiviral immune therapy.

Acknowledgements

We thank Dr. Y. Ikeda (Mayo clinic college of Medicine, USA) for the plasmid encoding rhesus and human TRIM5α harboring R437C mutation and for helpful advice. We are grateful to Dr. T. Shioda (Osaka University, Japan) for the gift of plasmid encoding human and AGM TRIM5α. We thank Dr. S. Okura and G. Towers (University college London, UK) for the pLNCX-GFP, pCIG3N and pCIG3B plasmids, Dr. T. Kitamura (University of Tokyo, Japan) for the MX-puro vector, Dr. K. Koyanagi (Kyoto University) for the pYK-JRCSF, Dr. A. Adachi (Tokushima University) for the pNL4-3, Dr. Mori (National Institute of Infectious Disease) for the pSIVmac239, Dr. Miura (Kyoto University) for the pSA212, AIDS Research and Reference Reagent Program for the p89.6, and Dr. K. Ikuta (Osaka University, Japan) for the mouse anti-HIV-1 Gag antibody. This work

was supported by grants from the Ministry of Education, Culture, Sports, Science, and Technology and the Ministry of Health, Labor and Welfare, Japan.

Appendix. Supplementary material

Supplementary data associated with this article can be found in the online version at doi:10.1016/j.micinf.2010.05.004.

References

[1] A.M. Sheehy, N.C. Gaddis, J.D. Choi, M.H. Malim, Isolation of a human gene that inhibits HIV-1 infection and is suppressed by the viral Vif protein. Nature 418 (2002) 646–650.
[2] H.L. Wiegand, B.P. Doehle, H.P. Bogerd, B.R. Cullen, A second human antiretroviral factor, APOBEC3F, is suppressed by the HIV-1 and HIV-2 Vif proteins. EMBO J. 23 (2004) 2451–2458.
[3] A. Takaori-Kondo, APOBEC family proteins: novel antiviral innate immunity. Int. J. Hematol. 83 (2006) 213–216.
[4] R. Goila-Gaur, K. Strebel, HIV-1 Vif, APOBEC, and intrinsic immunity. Retrovirology 5 (2008) 51.
[5] S.J. Neil, T. Zang, P.D. Bieniasz, Tetherin inhibits retrovirus release and is antagonized by HIV-1 Vpu. Nature 451 (2008) 425–430.
[6] P.D. Bieniasz, Intrinsic immunity: a front-line defense against viral attack. Nat. Immunol. 5 (2004) 1109–1115.
[7] M. Emerman, How TRIM5alpha defends against retroviral invasions. Proc. Natl. Acad. Sci. U.S.A. 103 (2006) 5249–5250.
[8] R. Sakuma, A.A. Mael, Y. Ikeda, Alpha interferon enhances TRIM5alpha-mediated antiviral activities in human and rhesus monkey cells. J. Virol. 81 (2007) 10201–10206.
[9] G. Peng, K.J. Lei, W. Jin, T. Greenwell-Wild, S.M. Wahl, Induction of APOBEC3 family proteins, a defensive maneuver underlying interferon-induced anti-HIV-1 activity. J. Exp. Med. 203 (2006) 41–46.
[10] M.J. Perron, M. Stremlau, M. Lee, H. Javanbakht, B. Song, J. Sodroski, The human TRIM5alpha restriction factor mediates accelerated uncoating of the N-tropic murine leukemia virus capsid. J. Virol. 81 (2007) 2138–2148.
[11] M. Stremlau, M. Perron, M. Lee, Y. Li, B. Song, H. Javanbakht, F. Diaz-Griffero, D.J. Anderson, W.I. Sundquist, J. Sodroski, Specific recognition and accelerated uncoating of retroviral capsids by the TRIM5alpha restriction factor. Proc. Natl. Acad. Sci. U.S.A. 103 (2006) 5514–5519.
[12] D. Perez-Caballero, T. Hatziioannou, F. Zhang, S. Cowan, P.D. Bieniasz, Restriction of human immunodeficiency virus type 1 by TRIM-CypA occurs with rapid kinetics and independently of cytoplasmic bodies, ubiquitin, and proteasome activity. J. Virol. 79 (2005) 15567–15572.
[13] D. Perez-Caballero, T. Hatziioannou, A. Yang, S. Cowan, P.D. Bieniasz, Human tripartite motif 5alpha domains responsible for retrovirus restriction activity and specificity. J. Virol. 79 (2005) 8969–8978.
[14] T. Hatziioannou, D. Perez-Caballero, S. Cowan, P.D. Bieniasz, Cyclophilin interactions with incoming human immunodeficiency virus type 1 capsids with opposing effects on infectivity in human cells. J. Virol. 79 (2005) 176–183.
[15] L. Berthoux, S. Sebastian, E. Sokolskaja, J. Luban, Lv1 inhibition of human immunodeficiency virus type 1 is counteracted by factors that stimulate synthesis or nuclear translocation of viral cDNA. J. Virol. 78 (2004) 11739–11750.
[16] X. Wu, J.L. Anderson, E.M. Campbell, A.M. Joseph, T.J. Hope, Proteasome inhibitors uncouple rhesus TRIM5alpha restriction of HIV-1 reverse transcription and infection. Proc. Natl. Acad. Sci. U.S.A. 103 (2006) 7465–7470.
[17] R. Sakuma, J.A. Noser, S. Ohmine, Y. Ikeda, Rhesus monkey TRIM5alpha restricts HIV-1 production through rapid degradation of viral Gag polyproteins. Nat. Med. 13 (2007) 631–635.
[18] F. Zhang, D. Perez-Caballero, T. Hatziioannou, P.D. Bieniasz, No effect of endogenous TRIM5alpha on HIV-1 production. Nat. Med. 14 (2008) 235–236 (author reply 236–238).
[19] M. Stremlau, M. Perron, S. Welikala, J. Sodroski, Species-specific variation in the B30.2(SPRY) domain of TRIM5alpha determines the potency of human immunodeficiency virus restriction. J. Virol. 79 (2005) 3139–3145.
[20] B. Song, B. Gold, C. O'Huigin, H. Javanbakht, X. Li, M. Stremlau, C. Winkler, M. Dean, J. Sodroski, The B30.2(SPRY) domain of the retroviral restriction factor TRIM5alpha exhibits lineage-specific length and sequence variation in primates. J. Virol. 9 (2005) 6111–6121.
[21] R. Sakuma, S. Ohmine, Y. Ikeda, Determinants for the rhesus monkey TRIM5{alpha}-mediated block of the late phase of HIV-1 replication. J. Biol. Chem. (2009).
[22] X. Wei, J.M. Decker, H. Liu, Z. Zhang, R.B. Arani, J.M. Kilby, M.S. Saag, X. Wu, G.M. Shaw, J.C. Kappes, Emergence of resistant human immunodeficiency virus type 1 in patients receiving fusion inhibitor (T-20) monotherapy. Antimicrob. Agents. Chemother. 46 (2002) 1896–1905.
[23] S. Morita, T. Kojima, T. Kitamura, Plat-E: an efficient and stable system for transient packaging of retroviruses. Gene. Ther. 7 (2000) 1063–1066.
[24] M. Onishi, T. Nosaka, K. Misawa, A.L. Mui, D. Gorman, M. McMahon, A. Miyajima, T. Kitamura, Identification and characterization of a constitutively active STAT5 mutant that promotes cell proliferation. Mol. Cell Biol. 18 (1998) 3871–3879.
[25] Y. Iwakura, T. Shioda, M. Tosu, E. Yoshida, M. Hayashi, T. Nagata, H. Shibuta, The induction of cataracts by HIV-1 in transgenic mice. AIDS 6 (1992) 1069–1075.
[26] A. Adachi, H.E. Gendelman, S. Koenig, T. Folks, R. Willey, A. Rabson, M.A. Martin, Production of acquired immunodeficiency syndrome-associated retrovirus in human and nonhuman cells transfected with an infectious molecular clone. J. Virol. 59 (1986) 284–291.
[27] Y. Koyanagi, S. Miles, R.T. Mitsuyasu, J.E. Merrill, H.V. Vinters, I.S. Chen, Dual infection of the central nervous system by AIDS viruses with distinct cellular tropisms. Science 236 (1987) 819–822.
[28] H. Kestler, T. Kodama, D. Ringler, M. Marthas, N. Pedersen, A. Lackner, D. Regier, P. Sehgal, M. Daniel, N. King, et al., Induction of AIDS in rhesus monkeys by molecularly cloned simian immunodeficiency virus. Science 248 (1990) 1109–1112.
[29] R. Shibata, T. Miura, M. Hayami, H. Sakai, K. Ogawa, T. Kiyomasu, A. Ishimoto, A. Adachi, Construction and characterization of an infectious DNA clone and of mutants of simian immunodeficiency virus isolated from the African green monkey. J. Virol. 64 (1990) 307–312.
[30] K. Peden, M. Emerman, L. Montagnier, Changes in growth properties on passage in tissue culture of viruses derived from infectious molecular clones of HIV-1LAI, HIV-1MAL, and HIV-1ELI. Virology 185 (1991) 661–672.
[31] J. Katahira, T. Ishizaki, H. Sakai, A. Adachi, K. Yamamoto, H. Shida, Effects of translation initiation factor eIF-5A on the functioning of human T-cell leukemia virus type I Rex and human immunodeficiency virus Rev inhibited trans dominantly by a Rex mutant deficient in RNA binding. J. Virol. 69 (1995) 3125–3133.
[32] S. Tahara-Hanaoka, K. Sudo, H. Ema, H. Miyoshi, H. Nakauchi, Lentiviral vector-mediated transduction of murine CD34(-) hematopoietic stem cells. Exp. Hematol. 30 (2002) 11–17.
[33] M. Bock, K.N. Bishop, G. Towers, J.P. Stoye, Use of a transient assay for studying the genetic determinants of Fv1 restriction. J. Virol. 74 (2000) 7422–7430.
[34] K. Ikuta, C. Morita, S. Miyake, T. Ito, M. Okabayashi, K. Sano, M. Nakai, K. Hirai, S. Kato, Expression of human immunodeficiency virus type 1 (HIV-1) gag antigens on the surface of a cell line persistently infected with HIV-1 that highly expresses HIV-1 antigens. Virology 170 (1989) 408–417.
[35] X. Li, Y. Li, M. Stremlau, W. Yuan, B. Song, M. Perron, J. Sodroski, Functional replacement of the RING, B-box 2, and coiled-coil domains of tripartite motif 5alpha (TRIM5alpha) by heterologous TRIM domains. J. Virol. 80 (2006) 6198–6206.

[36] Z. Keckesova, L.M. Ylinen, G.J. Towers, The human and African green monkey TRIM5alpha genes encode Ref1 and Lv1 retroviral restriction factor activities. Proc. Natl. Acad. Sci. U.S.A. 101 (2004) 10780–10785.
[37] M.J. Perron, M. Stremlau, B. Song, W. Ulm, R.C. Mulligan, J. Sodroski, TRIM5alpha mediates the postentry block to N-tropic murine leukemia viruses in human cells. Proc. Natl. Acad. Sci. U.S.A. 101 (2004) 11827–11832.
[38] M.W. Yap, S. Nisole, C. Lynch, J.P. Stoye, Trim5alpha protein restricts both HIV-1 and murine leukemia virus. Proc. Natl. Acad. Sci. U.S.A. 101 (2004) 10786–10791.
[39] M.W. Yap, S. Nisole, J.P. Stoye, A single amino acid change in the SPRY domain of human Trim5alpha leads to HIV-1 restriction. Curr. Biol. 15 (2005) 73–78.
[40] Y. Li, X. Li, M. Stremlau, M. Lee, J. Sodroski, Removal of arginine 332 allows human TRIM5alpha to bind human immunodeficiency virus capsids and to restrict infection. J. Virol. 80 (2006) 6738–6744.
[41] F. Diaz-Griffero, M. Perron, K. McGee-Estrada, R. Hanna, P.V. Maillard, D. Trono, J. Sodroski, A human TRIM5alpha B30.2/SPRY domain mutant gains the ability to restrict and prematurely uncoat B-tropic murine leukemia virus. Virology 378 (2008) 233–242.
[42] P.V. Maillard, S. Reynard, F. Serhan, P. Turelli, D. Trono, Interfering residues narrow the spectrum of MLV restriction by human TRIM5alpha. PLoS Pathog. 3 (2007) e200.
[43] E.C. Speelmon, D. Livingston-Rosanoff, S.S. Li, Q. Vu, J. Bui, D.E. Geraghty, L.P. Zhao, M.J. McElrath, Genetic association of the antiviral restriction factor TRIM5alpha with human immunodeficiency virus type 1 infection. J. Virol. 80 (2006) 2463–2471.
[44] E.E. Nakayama, W. Carpentier, D. Costagliola, T. Shioda, A. Iwamoto, P. Debre, K. Yoshimura, B. Autran, S. Matsushita, I. Theodorou, Wild type and H43Y variant of human TRIM5alpha show similar anti-human immunodeficiency virus type 1 activity both in vivo and in vitro. Immunogenetics 59 (2007) 511–515.
[45] D. van Manen, M.A. Rits, C. Beugeling, K. van Dort, H. Schuitemaker, N.A. Kootstra, The effect of Trim5 polymorphisms on the clinical course of HIV-1 infection. PLoS Pathog 4 (2008) e18.
[46] J.N. Torimiro, H. Javanbakht, F. Diaz-Griffero, J. Kim, J.K. Carr, M. Carrington, J. Sawitzke, D.S. Burke, N.D. Wolfe, M. Dean, J. Sodroski, A rare null allele potentially encoding a dominant-negative TRIM5alpha protein in Baka pygmies. Virology 391 (2009) 140–147.
[47] L. Carthagena, M.C. Parise, M. Ringeard, M.K. Chelbi-Alix, U. Hazan, S. Nisole, Implication of TRIM alpha and TRIMCyp in interferon-induced anti-retroviral restriction activities. Retrovirology 5 (2008) 59.

Vaccine 27 (2009) 966–971

Contents lists available at ScienceDirect

Vaccine

journal homepage: www.elsevier.com/locate/vaccine

Immunogenicity of newly constructed attenuated vaccinia strain LC16m8Δ that expresses SIV Gag protein

Hajime Suzuki[a], Minoru Kidokoro[b], Ismael Ben Fofana[a,1], Takashi Ohashi[a], Tomotaka Okamura[c], Kazuhiro Matsuo[c,2], Naoki Yamamoto[c], Hisatoshi Shida[a,*]

[a] Institute for Genetic Medicine, Hokkaido University, Kita-15, Nishi-7, Kita-ku, Sapporo 060-0815, Japan
[b] Department of Virology III, National Institute of Infectious Diseases, 4-7-1 Gakuen, Musashimurayama, Tokyo 208-0011, Japan
[c] AIDS Research Center, National Institute of Infectious Diseases, Shinjuku-ku, Tokyo 162-8640, Japan

ARTICLE INFO

Article history:
Received 14 August 2008
Received in revised form
23 November 2008
Accepted 6 December 2008
Available online 7 January 2009

Keywords:
SIV gag
Vaccinia m8Δ
IFN-γ-producing T cells

ABSTRACT

We developed the method to efficiently construct recombinant vaccinia viruses based on LC16m8Δ strain that can replicate in mammalian cells but is still safe in human. Immunization in a prime-boost strategy using DNA and LC16m8Δ expressing SIV Gag elicited 7–30-fold more IFN-γ-producing T cells in mice than that using DNA and non-replicating vaccinia DIs recombinant strain. As the previous study on the DNA-prime and recombinant DIs-boost anti-SIV vaccine showed protective efficacy in the macaque model [Someya K, Ami Y, Nakasone T, Izumi Y, Matsuo K, Horibata S, et al. Induction of positive cellular and humoral responses by a prime-boost vaccine encoded with simian immunodeficiency virus gag/pol. J Immunol 2006;176(3):1784–95], LC16m8Δ would have potential as a better recombinant viral vector for HIV vaccine.

1. Introduction

As vehicles for delivering antigens of HIV-1, replication-defective viral vectors have been extensively studied because of their safety. For example adenovirus and vaccinia virus-based vectors expressing Gag, Nef, and other components of HIV-1 have been evaluated in monkeys [1,3] and human trials [2,4,5]. They, however, generally have not induced sufficient level of immunity nor protected human from HIV-1 infection although they elicited considerable anti HIV/SIV immunities in animal models [6]. Moreover, controversial results have been reported on containment of challenged viruses depending on SIV or SHIV, a hybrid virus between HIV-1 and SIV, in monkey models [1,7]. Therefore more effective vehicles may be needed for HIV vaccine development.

Replication-competent vaccinia virus that has been proven to be safe in human vaccination against small pox could be a good candidate for a better vehicle. Vaccinia LC16m8 strain has been shot to 100,000 people without any serious adverse effects [8]. The LC16m8, however, has been found to be genetically unstable and to generate spontaneously more virulent revertants from stock of LC16m8 viruses. To improve LC16m8, we identified the B5R gene responsible for the reversion, and constructed genetically stable LC16m8Δ, which is essentially as same as LC16m8 in antigenicity and safety in mice, and approximately 1000-fold more immunogenic than non-replicating vaccinia, MVA strain. In particular, LC16m8Δ never elicited any symptoms in severe combined immunodeficiency disease mice even at 10^7 pfu dose [9]. Therefore LC16m8Δ could be a better vehicle for vaccines against HIV and other human diseases.

Gag proteins of HIV-1 and SIV are major antigens to elicit cytotoxic T lymphocyte (CTL) responses. Activity of anti Gag CTL in HIV-1-infected people inversely correlates with their viral loads [10]. In some monkey experiments of SIV infection, the strength of anti Gag CTL has been reported to correlate with the containment of SIV [11]. Therefore, we constructed LC16m8Δ that expresses the *gag* gene of SIVmac239 to compare its ability to elicit anti Gag immunity with replication-defective vaccinia virus DIs strain, which has been reported to be immunogenically similar to MVA [12], and to evaluate its potential as a recombinant vector for HIV vaccine development.

During the course of constructing LC16m8Δ-based recombinant viruses, we encountered a drawback, such as inefficient incorporation of the foreign gene by conventional method in which an *in vivo* recombination process is involved. Therefore, in this paper we firstly describe our new device including construction of a new strain m8Δvnc110, which prompts construction of m8Δ express-

* Corresponding author. Tel.: +81 11 706 7543; fax: +81 11 706 7543.
E-mail address: hshida@igm.hokudai.ac.jp (H. Shida).
[1] Present address: Microbiology Division, New England Primate Research Center, Harvard Medical School, One Pine Hill Drive, Southborough, MA 01772 USA.
[2] Present address: Research and Development Department, Japan BCG Laboratory, 3-1-5 Matsuyama, Kiyose, Tokyo 204-0022, Japan.

0264-410X/$ – see front matter © 2008 Elsevier Ltd. All rights reserved.
doi:10.1016/j.vaccine.2008.12.015

ing the *gag* gene of SIV by *in vitro* ligation of the vaccinia genome with foreign DNA.

2. Materials and methods

2.1. Cells and viruses

Rabbit RK13 cells were cultured in RPMI1640 supplemented with 10% FCS. Human HeLa, mouse L929, NIH3T3, hamster BHK, and primary chicken embryo fibroblast (CEF) cells were maintained in DMEM supplemented with 10% FCS. Canarypox virus (a kind gift of National Institute of Animal Health) [13], and LC16m8Δ [9] and DIs [14] strains of vaccinia virus were used. Viral titers were calculated on the basis of the number of plaques on CEF. The titer of LC16m8Δ was similar when titrated on RK13 and CEF monolayers.

2.2. Construction of pJWSIVgag

To construct the plasmid that expresses the SIV *gag* gene under the cytomegalovirus promoter, the *gag* coding region was amplified with a pair of primer SIVGAGF1 (GCCAAGCTTGCCACC-ATGGGCGTGAGAAACTCCGTCTTGTCAGG; the underlined sequence is HindIII site) and SIVGAGR1 (CGCGCCCGGGCTACTGGT CTCCTC-CAAAGAGAGAATTGAGGTGCAGC; the underlined sequence is XmaI site) using pSIVmac239 [15] as a template under the condition: 2 min at 94 °C, 20 cycles of 30 s at 94 °C, 60 s at 60 °C, 2 min at 72 °C, and a final extension for 5 min at 72 °C. The *gag* fragment generated was digested with HindIII and XmaI, and then ligated with the enzyme-digested pJW322, which harbors the cytomegalovirus promoter derived from pJW4303 [16] (a kind gift of Dr. Y. Takebe).

2.3. Construction of m8Δvnc110

To generate a transfer plasmid pVNC110, the vnc/KE sequence (5′-GGTACCCGCCCGGGCCGGACCGGCCGGCCGAATTC-3′) containing four restriction enzyme sites (SrfI, SfiI, RsrII, and FseI), which are not present in the vaccina virus genomes, was inserted between KpnI and EcoRI sites of pSFJ1-10, which harbors a strong composite promoter consisting of the cowpox A-type inclusion body (ATI) and multiple mutated-p7.5 promoters (PSFJ1-10 promoter), which are sandwiched with the segments of the vaccinia hemagglutinin (*HA*) gene [17,18]. pVNC110 resultant was verified by sequencing to harbor these sites downstream of PSFJ1-10 promoter, which is sandwiched by the segments of the vaccinia *HA* gene.

Next, we transfected 1.5 μg of pVNC110 to 1×10^5 BHK cells, which had been infected with LC16m8Δ at 0.05 moi, to construct m8Δvnc110. After the culture at 33 °C for 2 days, the progeny viruses were harvested and their plaques were formed on RK13 cell monolayer. The candidate viruses were selected on the basis of HA^- phenotype [19]. To ascertain whether the virus contains the expected sequences of pVNC110 in the *HA* gene, the virus-enriched fraction was prepared by disruption of the infected cells by repeated freeze and thaw followed by clarification by low speed centrifugation and concentration by centrifugation at 15,000 rpm for 30 min in microcentrifuge at 4 °C. Then, it was used as a template for PCR with a pair of the primers vvHA867s (GGATC-TACACATTCACCAGA) and vvHA1009as (CTAGTGTATGTGACGGTGT), the sequences of which were present in the *HA* gene, under the condition: 2 min at 94 °C, 30 cycles of 30 s at 94 °C, 60 s at 54 °C, 60 s at 72 °C, and a final extension for 5 min at 72 °C. Virus containing the sequence of VNC110 produced a 1 kb fragment of PCR product.

2.4. Construction of m8ΔSIVgag

Viral particles of m8ΔVNC110 were purified by method including banding in sucrose gradient centrifugation [20], and then viral DNA was isolated by phenol extraction method. The vaccinia DNA was digested with CpoI and FseI followed by purification with phenol extraction and ethanol precipitation. The *gag* region in SIVmac239 genome was amplified by PCR using pSIVmac239 [15] as a template with a pair of the primers CPO-SIV gag f2 (TTTCGGACCGCCACCATGGGCGTGAGAAACTCCGTCTTG; underlined sequence is CpoI site) and FSE-SIV gag r1 (TATGGCCGGCCTAC-TGGTCTCCTCCAAAGAGAGA; underlined sequence is FseI site) under the condition: 2 min at 94 °C, 20 cycles of 30 s at 94 °C, 60 s at 60 °C, 2 min at 72 °C, and a final extension for 10 min at 72 °C. The gag fragment was digested with CpoI and FseI followed by purification with PCR purification kit (Qiagen, Hilden, Germany). The digested vaccinia genome (5 μg) and gag fragment (0.3 μg) were ligated using a ligation kit (Takara, Otsu, Japan) according to the manual, purified by phenol extraction and concentrated by ethanol precipitation. The ligated DNA was transfected with lipofectamine LTX (Invitrogen, Carlsbad, USA) to 3.5×10^5 BHK cells that had been infected at 10 moi with canarypox virus. Usage of avipox viruses as a helper virus has been well established [21]. After 2 days culture at 33 °C, the progeny viruses were harvested by repeated freeze and thaw and titrated on the monolayer of RK13 cells. m8ΔSIVgag was cloned from single plaque and its homogeneity was evaluated by staining the plaques with sera of monkey infected with SIVmac239 and alkaline phosphatase-conjugated anti monkey IgG antibody followed by NBT/BCIP coloring reaction. All plaques were positively stained.

2.5. Construction of rDIs/PSFJ/SIVgag

To construct a complementary transfer vector for the deleted region of DIs, we used a pDIsgptmH5 plasmid (a kind gift of Dr. K. Ishii) that possesses both the modified H5 promoter and the *E. coli* guanine phosphoribosyltransferase (gpt) gene driven by a P7.5 promoter, which are sandwiched with the DIs fragments adjacent to the deleted region [22]. A vaccinia synthetic PSFJ1-10 promoter sequence [17] was amplified by PCR at 52 °C of the annealing temperature using a pair of the primers: PSFJ1-10s (ACATGCATGCATGAAGTTGAAGATGATG: underlined sequence is SphI site) and PSFJ1-10r (GATATCCTCGAGCA-GCACACCGTGCAATAAATT: underlined sequence is EcoRV and XhoI sites). To substitute the PSFJ1-10 promoter for the mH5 promoter, the PCR product was inserted into the SphI and EcoRV sites of pDIsgptmH5, generating pUC/DIs/PSFJ that could express the foreign antigen gene under the control of the PSFJ1-10 promoter. A DNA fragment encoding the full-length gag gene of SIVmac239 was amplified by PCR at 55 °C of the annealing temperature using a pair of the primers: gag-s (CCCCCCGGGATGGGCGTGAGAAACTCC: underlined sequence is SmaI site) and gag-r (CCGGAGCTCCTACTGGTCTCCTCCAAAGAG: underlined sequence is SacI site), and inserted into the SmaI and SacI sites of pUC/DIs/PSFJ to generate the transfer vector, named pUC/DIs/PSFJ/SIVgag. This plasmid (10 μg) was transfected by Gene-Pulser (Bio-Rad Laboratories, Inc. Hercules, USA) to CEF infected with DIs at 1.0 moi. Recombinant DIs clones expressing the SIV *gag* gene were selected in the presence of gpt [23].

2.6. Western blotting

m8ΔSIVgag and rDIs/PSFJ/SIVgag were infected to various cells at 3 or 5 moi and cultured for 24 h at 33 °C. Then the infected cells and culture medium were collected and their protein amounts were quantified by BCA assay. Appropriate amounts of the cell lysates and medium fraction indicated in the figure legends were subjected to 12% SDS-PAGE and immunologically detected using 500-fold-diluted sera from SIVmac239-infected monkey and alkaline phosphatase-conjugated anti monkey IgG antibody (Promega, Madison, USA) followed by NBT/BCIP coloring reaction.

2.7. Immunization

Seven-week-old female C57/BL6 mice were purchased from CLEA Co. Ltd. (Tokyo, Japan). Fifty microgram of pJWSIVgag was intramuscularly injected into the right and left quadriceps, and 1×10^6 pfu of vaccinia viruses were inoculated intrademally according to the schedule indicated in Figs. 3A and 4A. All mice were maintained according to the institutional animal care and the guidelines of Hokkaido University. The study was conducted in a biosafety level 2 facility under the approval of an institutional committee for biosafety and in accordance with the requirements of the World Health Organization.

2.8. Assay of cellular immune response by IFN-γ ELISPOT

SIV Gag specific IFN-γ producing cells were quantified 2 or 3 weeks after the final immunization using an ELISPOT kit for mouse IFN-γ (R&D Systems, Minneapolis, USA). The excised spleens were disrupted with a syringe plunger and passed through a cell strainer (Becton Dickinson, Franklin Lakes, USA). Isolated spleen cells were suspended at 10^6 cells/ml in RPMI 1640 medium supplemented with 10% fetal bovine serum, penicillin and streptomycin. Aliquots (100 μl) were plated into wells that were coated with anti-mouse IFN-γ antibody and stimulated with SIV Gag-specific 15 mer overlapping peptide pools (0.5 μg of peptides/10^5 cells) (A gift of AIDS Research and Reference Reagent program. Catalog #6204). Cells mock-stimulated with medium alone served as a negative control while cells treated with 50 ng/ml of phorbol 12-myristate (PMA) and 0.5 μg/ml of calcium ionomycin were used as a positive control to ascertain the number of viable T cells. After 24 h incubation, IFN-γ secreting cells were detected according to the manufacturer's instructions. Numbers of spot forming cells (SFC) were determined using the ImmunoScan Plate Reader with ImmunoSpot software (Cellular Technology Limited, Cleveland, USA).

2.9. Proliferation assays

Lymphocyte proliferation was measured by incorporation of BrdU into the stimulated-lymphocytes using cell proliferation ELISA BrdU kit (Roche Applied Science, Mannheim, Germany). Isolated spleen cells (1×10^5) were cultured in a 96-well assay plate (BD Falcon, Franklin Lakes, USA) in the presence or absence of recombinant SIV Gag protein (SIVmac251 p27; Advanced Biotechnologies, Inc., Columbia, USA) at 5.0 μg/ml for antigen-specific stimulation. The plates were incubated for 2 days at 37 °C, and then another 24 h in the presence of BrdU (100 μM). Uptake of BrdU was determined using luminometer (Wallac 1420; PerkinElmer, Branchburg, USA). The results were expressed as the stimulation index (SI), which was calculated as a ratio of relative light unit per second in the presence to that in the absence of the antigen.

2.10. Statistical analysis

Data were expressed as arithmetic mean ± standard error of means (mean ± S.E.M.). The data analysis was carried out by using Student's *t*-test (EXCEL version 11.5, Microsoft). A *P*-value of <0.05 was considered significant.

3. Results

3.1. Construction of m8ΔSIVgag

Fig. 1 illustrates the outline for construction of m8ΔSIVgag. Firstly we constructed m8ΔVNC110 strain by usual method in which pVNC110 was transfected to BHK cells that had been infected with LC16m8Δ. Resultant m8ΔVNC110 harbors PSFJ1-10 promoter followed by the multi-cloning sites containing the restriction enzyme sites which are not present in the vaccinia genome. To construct m8ΔSIVgag, the genomic DNA extracted from ΔVNC110 virions was digested with CpoI and FseI, which do not cut the other part of the vaccinia genome, and ligated with SIV *gag* fragment *in vitro*. Then the ligation mixture was transfected to BHK cells that had been infected with canarypox virus, which cannot replicate in mammalian cells. A clone, named m8ΔSIVgag3, that was isolated from one among six plaques formed by the progeny viruses produced SIV Gag protein judged by staining the plaques with sera derived from a SIV-infected monkey.

3.2. Comparison of Gag production by LC16m8Δ and DIs-based recombinants

Previously Honda's group constructed replication-deficient vaccinia DIs strain-based recombinant, which had immunogenicity similar to MVA-based recombinant [12]. We now compared by

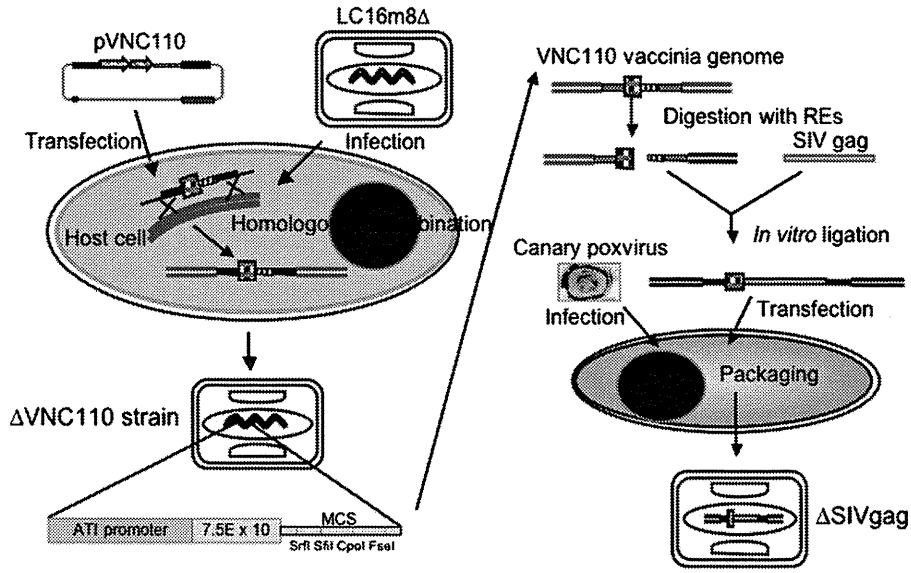

Fig. 1. Schematic presentation for construction of m8ΔSIVgag.

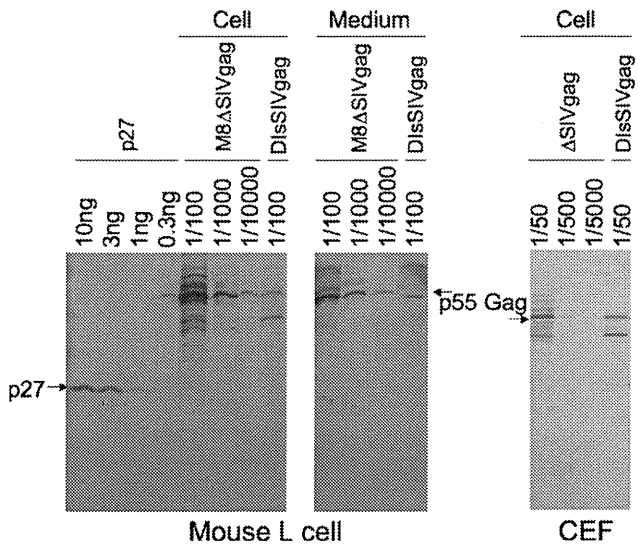

Fig. 2. Western blotting for p55 Gag produced by vaccinia recombinants. Appropriate fractions (1/50–1/10,000) of the cell lysates and medium prepared from m8ΔSIVgag- or rDIs/PSFJ/SIVgag-infected cells were subjected to Western blotting. One hundredth of the cell lysates contains approximately 1 μg of proteins.

Western blotting the amount of Gag protein produced by LC16m8Δ and DIs, both of which used the same promoter for expression of the foreign gene (Fig. 2). In mouse L cells, where DIs is not able to replicate, approximately 100-fold more amount of Gag protein was detected in both medium and cells infected at high multiplicity with m8ΔSIVgag than that in the cells infected with rDIs/PSFJ/SIVgag, whereas m8ΔSIVgag produced Gag protein just several fold more than rDIs/PSFJ/SIVgag in CEF in which both viruses replicate. In human HeLa, mouse NIH3T3, and rabbit RK13 cells m8ΔSIVgag again produced Gag protein 100-fold more than rDIs/PSFJ/SIVgag (data not shown). These results suggest that production of Gag is affected by not only the promoter just upstream of the foreign gene but also the replication capability of the vector virus.

3.3. Immunogenicity of LC16m8Δ and DIs-based recombinants

Next, we evaluated the immunogenicities of these recombinant viruses in mice by priming with plasmid pJWSIVgag expressing the *gag* gene followed by boosting with these recombinant viruses. Considering the preceding reports that viral vectors failed to elicit enough immunities in human although they were nicely antigenic in mice under optimal immunization schedule [4,24], we compared their immunogenicities under the suboptimal condition that includes two or three priming with pJWSIVgag followed by boosting once with 1×10^6 pfu of the recombinant viruses. We have assessed the number of IFN-γ producing cells by ELISPOT assay 2 weeks after a shot of the recombinant viruses, and found that sevenfold more cells were induced by prime-boost vaccination with pJWSIVgag and SIVm8Δgag than that of rDIs/PSFJ/SIVgag (Fig. 3). We also evaluated the induction of Gag specific IFN-γ producing cells by single immunization with pJWSIVgag, SIVm8Δgag or rDIs/PSFJ/SIVgag. In contrast to prime-boost regimen, significant positive spots were not detected by ELISPOT assay (data not shown). When assayed 3 weeks after final immunization with the viruses, differences were more prominent in that only one among four mice immunized with rDIs/PSFJ/SIVgag were ELISPOT positive com-

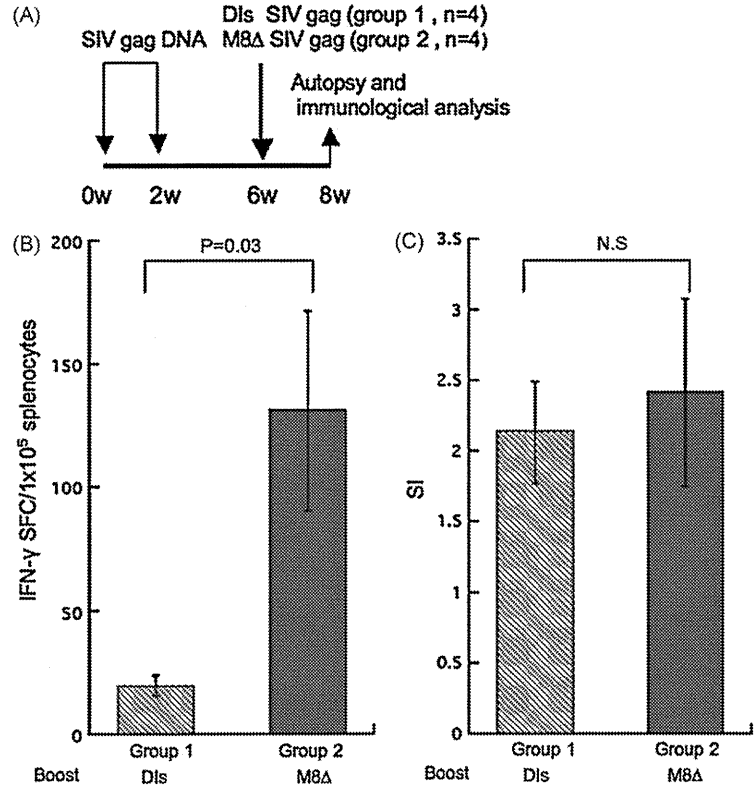

Fig. 3. Comparison of booster effect by m8ΔSIVgag and rDIs/PSFJ/SIVgag. (A) Schematic drawing of experimental design for immunization. Mice were immunized twice with SIVgag DNA followed by one boost with rDIs/PSFJ/SIVgag (group 1) or m8ΔSIVgag (group 2). (B) Frequency of SIV Gag-specific IFN-γ-producing cells in immunized mice. Spleen cells were stimulated with pooled SIV Gag peptides, and IFN-γ-producing cells were detected by IFN-γ-specific ELISPOT assays. Data are expressed as the mean number of SFC per 10^5 splenocytes ± S.E.M. (C) Induction of SIV Gag-specific lymphocyte proliferatives response. Spleen cells were cultured in the presence or absence of SIV p27 antigen, and incorporation of BrdU was measured as described in Section 2. Proliferative responses were presented as the value of the stimulation index (SI). Data are mean ± S.E.M. N.S. means not significant.

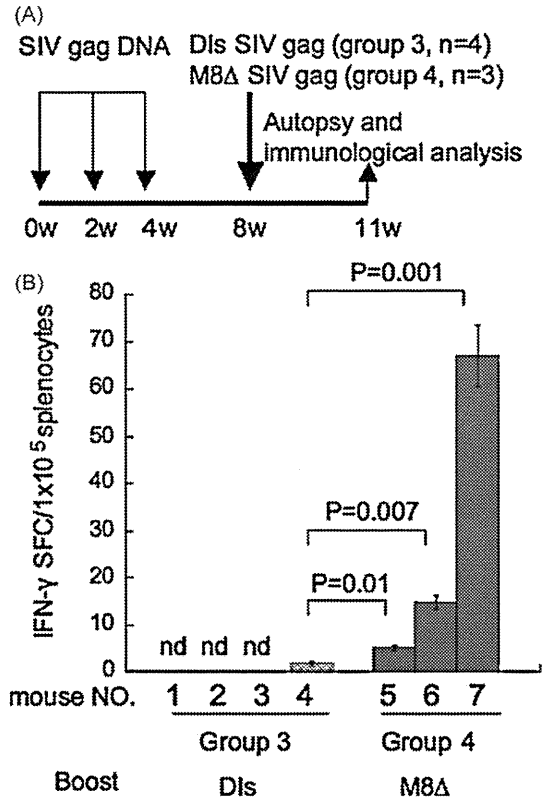

Fig. 4. Comparison of immunogenicities of m8ΔSIVgag and rDIs/PSFJ/SIVgag. (A) Schematic drawing of experimental design for immunization. Mice were immunized three times with SIVgag DNA followed by one boost with rDIs/PSFJ/SIVgag (group 3) or m8ΔSIVgag (group 4). (B) Frequencies of SIV Gag-specific IFN-γ-producing cells in individual immunized mice were presented as the number of SFC per 10^5 splenocytes. SFC of individual mouse was counted in triplicate and presented as the means ± S.E.M.

pared with all positive mice with m8Δgag and average of ELSPOT was approximately 30-fold more in mice immunized with m8Δgag than rDIs/PSFJ/SIVgag (Fig. 4). To monitor the sensitivity of ELISPOT assays, we always included positive controls that were splenocytes stimulated with PMA and ionomycin, and ascertained that they produced 300–500 spots/10^5 splenocytes in every experiment (data not shown).

Proliferation capacities of the lymphocytes derived from the immunized mice were also compared based on BrdU incorporation. Splenocytes from both immunized groups showed low levels of T-cell proliferation in response to stimulation with SIV Gag protein (Fig. 3). But we did not find significant difference between the mice immunized by either virus in contrast to the results of ELISPOT assay described above.

4. Discussion

In this study, we devised a new method involving *in vitro* ligation to efficiently construct recombinant vaccinia viruses expressing the foreign genes. We could construct SIV Gag expressing m8Δ only by this technique but not by the conventional method, which involves *in vivo* ligation. Moreover, we have successfully constructed two additional recombinant viruses expressing the chimeric genes, which contain rat MHC class I with an epitope sequence fused with β2 microglobulin. Approximately 60% of the progeny viruses expressed the transgenes even when no methods were used to enrich the recombinants (They will be published elsewhere.), suggesting that this new technique is generally applicable to construct m8Δ-based recombinant viruses.

Here, using the same promoter in both recombinant DIs and LC16m8Δ strains of vaccinia, we have demonstrated a much more efficient expression of SIV Gag transgene by the latter in several mammalian cells, which were infected at a high dose of inoculum. In contrast, less difference was observed in the level of Gag protein expression in CEF probably because both recombinant viruses propagated at comparable level in this cell type. These results suggest that vaccinia viruses, which propagate better, could provide more efficacious expression of immunogens of interest.

The propagation capability and related efficacy of Gag production by these recombinant vaccinia viruses may reflect their immunogenicity. IFN-γ producing T cells evaluated by ELISPOT were more efficiently elicited by m8ΔSIVGag and lasted longer than those by rDIs/PSFJ/SIVgag. Since several non-replicating vaccinia virus vectors including DIs, MVA, and NYVAC have been shown to be similarly immunogenic in mice [12,25], replication-competent vector such as LC16m8Δ may be more immunogenic than general non-replicating vectors. Since anti-SIV vaccination comprising the DNA-prime and recombinant DIs-boost has been reported to elicit protective immunity in the macaque model [26], it may be expected that m8ΔSIVGag would confer better protection against SIV challenge.

Our results are in contrast with reports by Hirsch et al., that showed similar level of immunogenicity between SIV Gag recombinant MVA and a replication-competent vaccinia vectors when a very high dose of vaccine was applied [27]. However, it should be important to evaluate the immunogenicities of vaccinia recombinants under the suboptimal immunization schedule, including a single boost with a low dose of vaccinia recombinants, which was adopted in this study, given that unsuccessful outcome of the human trials by the vaccines [2,4] that had been appreciated based on protective immune responses elicited by optimal immunization schedule in model animals [24,28].

Mucosal immunity has been suggested to be important for protection against HIV, because it sexually transmit in most cases. Since history of exposure of replicating virus in mucosal tissues has been reported to prime the mucosal immune system and lead to the induction of secretary IgA [29], it is expected that LC16m8Δ vaccination via the mucosal route may induce effective mucosal immunity. Moreover, replicating adenovirus vector has also been reported to be more effective than non-replicating one [30].

In contrast to the more efficient induction of IFN-γ producing T cells by m8ΔSIVGag, the Gag-specific lymphocyte proliferation responses were similarly elicited by both recombinants. Vaccinia viruses produce various kinds of immunomodulatory factors, which may tend to elicit uneven immunities [31]. Therefore, it is conceivable that quantitative and qualitative differences of the factors produced by LC16m8Δ and DIs strains may cause the diverged immune responses.

In summary, we devised an efficient method to construct a recombinant virus based on LC16m8Δ and evaluated it as a vaccine candidate. This replication-competent virus vector showed merits for further development in the viewpoint of its ability to elicit enhanced cell-mediated and hopefully humoral and mucosal immune responses.

Acknowledgements

We thank A. Hirano and N. Mizuno for technical assistance. This work was supported by grants from the Ministry of Sports and Culture (Japan), and the Ministry of Health and Welfare (Japan). pJW4303, pUC/DIs/mH5, and the SIV-specific 15 mer overlapping peptide pools were kindly supplied by Dr. Y. Takebe (NIID), Dr. K. Ishii (NIID), and the NIH AIDS Research and Reference Reagent Program, respectively. A canarypox virus, a kind gift of National

Institute of Animal Health was obtained through Dr. S. Morikawa (NIID).

References

[1] Casimiro DR, Wang F, Schleif WA, Liang X, Zhang Z, Tobery TW, et al. Attenuation of simian immunodeficiency virus SIVmac239 infection by prophylactic immunization with DNA and recombinant adenoviral vaccine vectors expressing Gag. J Virol 2005;79(24):15547–55.

[2] Cox KS, Clair JH, Prokop MT, Sykes KJ, Dubey SA, Shiver JW, et al. DNAgag/Ad5gag and Ad5gag/Ad5gag vaccines induce distinct T cell response profiles. J Virol 2008;82(16):8161–71.

[3] Vogel TU, Reynolds MR, Fuller DH, Vielhuber K, Shipley T, Fuller JT, et al. Multispecific vaccine-induced mucosal cytotoxic T lymphocytes reduce acute-phase viral replication but fail in long-term control of simian immunodeficiency virus SIVmac239. J Virol 2003;77(24):13348–60.

[4] Goonetilleke N, Moore S, Dally L, Winstone N, Cebere I, Mahmoud A, et al. Induction of multifunctional human immunodeficiency virus type 1 (HIV-1)-specific T cells capable of proliferation in healthy subjects by using a prime-boost regimen of DNA- and modified vaccinia virus Ankara-vectored vaccines expressing HIV-1 Gag coupled to CD8 T-cell epitopes. J Virol 2006;80(10):4717–28.

[5] Harari A, Bart PA, Stöhr W, Tapia G, Garcia M, Medjitna-Rais E, et al. An HIV-1 clade C DNA prime, NYVAC boost vaccine regimen induces reliable, polyfunctional, and long-lasting T cell responses. J Exp Med 2008;205(1):63–77.

[6] Walker BD, Burton DR. Toward and AIDS Vaccine. Science 2008; 320(5877):760–4.

[7] Shiver JW, Fu TM, Chen L, Casimiro DR, Davies ME, Evans RK, et al. Replication-incompetent adenoviral vaccine vector elicits effective anti-immunodeficiency-virus immunity. Nature 2002;415(6869):331–5.

[8] Hashizume S, Yoshizawa H, Morita M, Suzuki K. Properties of attenuated mutant of vaccinia virus, LC16m8, derived from Lister strain. In: Ouinnan GV, editor. In Vaccinia viruses as Vectors for Vaccine Antigens. Amsterdam: Elsevier; 1985. p. 421–8.

[9] Kidokoro M, Tashiro M, Shida H. Genetically stable and fully effective smallpox vaccine strain constructed from highly attenuated vaccinia LC16m8. Proc Natl Acad Sci USA 2005;102(11):4152–7.

[10] Kiepiela P, Ngumbela K, Thobakgale C, Ramduth D, Honeyborne I, Moodley E, et al. CD8+ T-cell responses to different HIV proteins have discordant associations with viral load. Nat Med 2007;13(1):46–53.

[11] Matano T, Kobayashi M, Igarashi H, Takeda A, Nakamura H, Kano M, et al. Cytotoxic T lymphocyte-based control of simian immunodeficiency virus replication in a preclinical AIDS vaccine trial. J Exp Med 2004;199(12):1709–18.

[12] Okamura T, Someya K, Matsuo K, Hasegawa A, Yamamoto N, Honda M. Recombinant vaccinia DIs expressing simian immunodeficiency virus gag and pol in mammalian cells induces efficient cellular immunity as a safe immunodeficiency virus vaccine candidate. Microbiol Immunol 2006;50(12):989–1000.

[13] Amano H, Morikawa S, Shimizu H, Shoji I, Kurosawa D, Matsuura Y, et al. Identification of the canarypox virus thymidine kinase gene and insertion of foreign genes. Virology 1999;256(2):280–90.

[14] Ishii K, Ueda Y, Matsuo K, Matsuura Y, Kitamura T, Kato K, et al. Structural analysis of vaccinia virus DIs strain: application as a new replication-deficient viral vector. Virology 2002;302(2):433–44.

[15] Kestler H, Kodama T, Ringler D, Marthas M, Pedersen N, Lackner A, et al. Induction of AIDS in rhesus monkeys by molecularly cloned simian immunodeficiency virus. Science 1990;248(4959):1109–12.

[16] Lu S, Manning S, Arthos J. Antigen Engineering in DNA Immunization. Totowa, NJ: Humana Press; 1999. pp. 355–74.

[17] Jin NY, Funahashi S, Shida H. Constructions of vaccinia virus A-type inclusion body protein, tandemly repeated mutant 7.5 kDa protein, and hemagglutinin gene promoters support high levels of expression. Arch Virol 1994;138(3–4):315–30.

[18] Shida H, Tochikura T, Sato T, Konno T, Hirayoshi K, Seki M, et al. Effect of the recombinant vaccinia viruses that express HTLV-I envelope gene on HTLV-I infection. EMBO J 1987;6(11):3379–84.

[19] Shida H, Matsumoto S. Analysis of the hemagglutinin glycoprotein from mutants of vaccinia virus that accumulates on the nuclear envelope. Cell 1983;33(2):423–34.

[20] Joklik WK. The purification of four strains of poxvirus. Virology 1962;18:9–18.

[21] Scheiflinger F, Dorner F, Falkner FG. Construction of chimeric vaccinia viruses by molecular cloning and packaging. Proc Natl Acad Sci USA 1992;89(21):9977–81.

[22] Ishii K, Hasegawa H, Nagata N, Mizutani T, Morikawa S, Suzuki T, et al. Induction of protective immunity against severe acute respiratory syndrome coronavirus (SARS-CoV) infection using highly attenuated recombinant vaccinia virus DIs. Virology 2006;351(2):368–80.

[23] Wolffe EJ, Isaacs SN, Moss B. Deletion of the vaccinia virus B5R gene encoding a 42-kilodalton membrane glycoprotein inhibits extracellular virus envelope formation and dissemination. J Virol 1993;67(8):4732–41.

[24] Hanke T, Blanchard TJ, Schneider J, Hannan CM, Becker M, Gilbert SC, et al. Enhancement of MHC class I-restricted peptide-specific T cell induction by a DNA prime/MVA boost vaccination regime. Vaccine 1998;16(5):439–45.

[25] Gómez CE, Nájera JL, Jiménez EP, Jiménez V, Wagner R, Graf M, et al. Head-to-head comparison on the immunogenicity of two HIV/AIDS vaccine candidates based on the attenuated poxvirus strains MVA and NYVAC co-expressing in a single locus the HIV-1BX08 gp120 and HIV-1(IIIB) Gag-Pol-Nef proteins of clade B. Vaccine 2007;25(15):2863–85.

[26] Someya K, Ami Y, Nakasone T, Izumi Y, Matsuo K, Horibata S, et al. Induction of positive cellular and humoral responses by a prime-boost vaccine encoded with simian immunodeficiency virus gag/pol. J Immunol 2006;176(3):1784–95.

[27] Hirsch VM, Fuerst TR, Sutter G, Carroll MW, Yang LC, Goldstein S, et al. Patterns of viral replication correlate with outcome in simian immunodeficiency virus (SIV)-infected macaques: effect of prior immunization with a trivalent SIV vaccine in modified vaccinia virus Ankara. J Virol 1996;70(6):3741–52.

[28] Juillard V, Villefroy P, Godfrin D, Pavirani A, Venet A, Guillet JG. Long-term humoral and cellular immunity induced by a single immunization with replication-defective adenovirus recombinant vector. Eur J Immunol 1995;25(12):3467–73.

[29] Herremans TM, Reimerink JH, Buisman AM, Kimman TG, Koopmans MP. Induction of mucosal immunity by inactivated poliovirus vaccine is dependent on previous mucosal contact with live virus. J Immunol 1999;162(8):5011–8.

[30] Peng B, Wang LR, Gómez-Román VR, Davis-Warren A, Montefiori DC, Kalyanaraman VS, et al. Replicating rather than nonreplicating adenovirus-human immunodeficiency virus recombinant vaccines are better at eliciting potent cellular immunity and priming high-titer antibodies. J Virol 2005;79(16):10200–9.

[31] Seet BT, Johnston JB, Brunetti CR, Barrett JW, Everett H, Cameron C, et al. Poxviruses and immune evasion. Annu Rev Immunol 2003;21:377–423.

Regulation of the susceptibility of HIV-1 to a neutralizing antibody KD-247 by nonepitope mutations distant from its epitope

Mari Takizawa[a], Kosuke Miyauchi[a], Emiko Urano[a], Shigeru Kusagawa[a], Katsuhiko Kitamura[b], Satoshi Naganawa[c], Toshio Murakami[d], Mitsuo Honda[e], Naoki Yamamoto[f] and Jun Komano[a]

Objective: A humanized neutralizing antibody, KD-247, targets the V3 loop of HIV-1 Env. HIV-1 bearing the GPGR sequence at the V3 loop is potentially susceptible to KD-247. However, not all GPGR-positive HIV-1 isolates are neutralized by KD-247. We examined the potential mechanism by which the susceptibility of HIV-1 to KD-247-mediated neutralization is regulated.

Design: We searched for nonepitope neutralization regulatory (NNR) mutations that sensitize GPGR-bearing HIV-1_{AD8} to KD-247 and mapped the locations of such mutations relative to the V3 loop.

Methods: We generated a functional HIV-1_{AD8} Env library, and evaluated the viral susceptibility to KD-247 by measuring the half-inhibitory concentration (IC_{50}) to KD-247 on TZM-bl cell assay.

Results: We identified nine KD-247-sensitizing NNR mutations from 30 mutations in various regions of gp120, including the V1/V2 loop, C2, V3 loop, C4, and C5. They specifically affected KD-247-mediated neutralization, as they did not affect the b12-mediated neutralization. When combined, the KD-247-sensitizing NNR mutations additively sensitized the virus to KD-247 by up to 10 000 folds. The KD-247-sensitizing NNR mutations increased KD-247 binding to the virion. Notably, the NNR mutation in C4 coincides with the CD4-binding site of gp120.

Conclusion: Given that most of the KD-247-sensitizing NNR mutations are remote from V3 loop, it is reasonable to hypothesize that the steady-state, local conformation of the V3 loop is regulated by the interdomain contact of gp120. Our mutational analysis complements crystallographic studies by helping provide a better understanding of the steady-state conformation and the functional geometry of Env.

AIDS 2011, **25**:2209–2216

Keywords: envelope, HIV-1, KD-247, neutralization, steady-state conformation

Introduction

HIV-1 is a highly mutagenic virus. The viral envelope glycoprotein gp120/41 (Env) accumulates mutations to escape from the host humoral immunity. The study on HIV-1-neutralizing antibodies (Nabs) and the viral escape from Nab gives us insights into viral pathogenesis, structure–function relationship of Env, and AIDS vaccine design [1–8].

[a]AIDS Research Center, National Institute of Infectious Diseases, Tokyo, [b]Department of Public Health, Yokohama City University School of Medicine, Yokohama, [c]Infectious Disease Regulation Project, The Tokyo Metropolitan Institute of Medical Science, Tokyo, [d]The Chemo-Sero-Therapeutic Research Institute, Kumamoto, [e]Department of Pathology and Microbiology, Division of Microbiology, Nihon University School of Medicine, Tokyo, Japan, and [f]Department of Microbiology, Yong Loo Lin School of Medicine, National University of Singapore, Singapore.

Correspondence to Jun Komano, AIDS Research Center, National Institute of Infectious Diseases, 1-23-1 Toyama Shinjuku, Tokyo 162-8640, Japan.

Tel: +81 3 5285 1111; fax: +81 3 5285 5037; e-mail: ajkomano@nih.go.jp

Received: 8 September 2010; revised: 4 July 2011; accepted: 5 August 2011.

DOI:10.1097/QAD.0b013e32834bab68

ISSN 0269-9370 © 2011 Wolters Kluwer Health | Lippincott Williams & Wilkins

A humanized monoclonal Nab, KD-247, which is effective against half of clade B primary HIV-1 isolates, targets the third hypervariable (V3) loop, is an attractive AIDS vaccine target [1–3]. The epitope essential for KD-247-mediated neutralization is the conserved tetrapeptide sequence GPGR (HXB2 coordinate 312–315). A human monoclonal Nab 447–52D targets this same epitope [4]. Mutations in the GPGR sequence confer viral resistance to KD-247 [3,5,6]. Moreover, amino acid changes adjacent to the GPGR motif have also conferred viral resistance to KD-247 (e.g. H, R, and K at 311 position, or P at 316 position) [3]. Such mutations physically interfere with binding to the KD-247 epitope [3]. In the absence of such mutations, HIV-1 bearing the GPGR sequence at the V3 loop is potentially susceptible to KD-247. However, not all GPGR-positive HIV-1 isolates are neutralized by KD-247. The mechanism by which some of the GPGR-bearing viruses are resistant to KD-247 is not fully understood.

We addressed this sequence-neutralization susceptibility discordance by comparing the amino acid sequences of various HIV-1 primary isolates. We defined a virus as resistant to KD-247-mediated neutralization when the half-inhibitory concentration (IC_{50}) was higher than 100 μg/ml. We analyzed V3 loop amino acid sequences from 25 viruses positive for the GPGR epitope, including 11 KD-247-sensitive and 14 KD-247-resistant viruses. Along with the ELISA data in our previous report [3], we found that H304R contributes to KD-247 resistance. The H304R polymorphism accounted for 35.7% (five of 14 isolates) of the examples of sequence-neutralization susceptibility discordance, but all the viruses carrying H304R were CRF01_AE. We failed to identify any neutalization regulatory mutations in the clade B isolates. Additionally, the KD-247 prototype mouse monoclonal antibody C25 was unable to neutralize 17 GPGR-positive HIV-1 clade B primary isolates, even though C25 was able to bind their synthetic V3 loop peptides (unpublished observation). From these data, we postulated that the sequence-neutralization susceptibility discordance is due to non-epitope neutralization regulatory (NNR) mutations, especially remote from the V3 loop. Such NNR mutations would be positioned at certain key sites within the Env domains and regulate the steady-state conformation. NNR mutations have been predicted for 447–52D and other cross-reactive Nab [6–11]. To test this hypothesis, we examined 15 entire Env amino acid sequences of KD-247-sensitive and KD-247-resistant viruses. However, we were unable to identify amino acids associated with susceptibility to KD-247. This suggests that the heterologous virus approach is not sensitive enough to identify NNR mutations because the diversity of Env amino acid sequences is beyond the level of detection.

Here we employed a genetic approach to identify NNR mutations using the HIV-$1_{AD8/ADA}$ (AD8 hereafter), which displays the sequence-neutralization susceptibility discordance. The AD8 strain has been reported to be sensitive to 447–52D, which targets the same neutralization epitope as KD-247 within the V3 loop [10], suggesting that the GPGR epitope of the V3 loop is open to antibodies. We thought that this should help understand how the NNR mutations work. It does not contain insertions adjacent to the GPGR motif, as HIV-1_{HXB2} or HIV-1_{NL4-3} do (QR insertion before I and G) nor H304R. Only a few NNR mutations that make HIV-1 resistant to KD-247 have been reported in the V1/V2 loop [6]. In this work, we generated a functional AD8 Env library to identify many NNR mutations simultaneously that cause HIV-1 to become susceptible to KD-247. Through KD-247-sensitizing NNR mutations, we tried to understand the regulatory mechanism of the viral susceptibility to KD-247-mediated neutralization.

Materials and methods

Cells, viruses, and transfection

Cells were maintained in RPMI-1640 Medium (Sigma, St Louis, Missouri, USA) supplemented with 10% fetal bovine serum (FBS) (Japan Bioserum, Tokyo, Japan), 50 U/ml penicillin, and 50 μg/ml streptomycin (Invitrogen, Tokyo, Japan), at 37°C in a humidified 5% CO_2 atmosphere. Cells were transfected with Lipofectamine 2000 according to the manufacturer's protocol (Invitrogen). The other viruses and TZM-bl cells were obtained from the NIH AIDS Research and Reference Reagent Program.

Antibodies

KD-247 was provided by the Chemo-Sero-Therapeutic Research Institute, and b12 is a generous gift from Dr Burton (The Scripps Research Institute).

Cloning

AD8 Env was amplified by nested reverse-transcriptase-PCR using RNA extracted from the culture supernatant as a template (RNeasy mini kit; Qiagen, Hilden, Germany). The primers used were as follows. For the first PCR, the sense primer was 5′-ATG AAA CTT ACG GGG ATA CTT GGG-3′ (HXB2 nucleotide coordinates 5698–5721) and the antisense primer was 5′-GGT ACT AGC TTG AAG CAC CAT CC-3′ (HXB2 nucleotide coordinates 9236–9214); and for the nested PCR, the sense primer was 5′-ATA AGA ATT CTG CAA CAA CTG CTG-3′ (HXB2 nucleotide coordinates 5739–5762) and the antisense primer was 5′-TTC CAG GTC TCG AGA TGC TGC-3′ (HXB2 nucleotide coordinates 8910–8890). EcoRI-XhoI fragments of the PCR products were cloned into the corresponding restriction sites of pNL4–3. The *env* gene was sequenced using the following primers: 3479a, 5′-CTT GGG ATG TTG

ATG ATC TGT AGT GCT GTA GA-3′; 003A, 5′-AGC AGA AGA CAG TGG CAA TG-3′; 106A, 5′-CAT ACA TTA TTG TGC CCC GGC TGG-3′; 545A, 5′-GAC AAT TGG AGA AGT GAA TT-3′; and 5700, 5′-AGC CTG TGC CTC TTC AGC TAC CAC CGC TTG-3′.

Neutralization assay

To produce virus from proviral DNA, 293FT cells (Cat# R700–007; Invitrogen) grown in six-well plates were transfected with proviral DNA-encoding plasmid (1 μg) using Lipofectamine 2000, and replated into a six-well plate at 4–6 h posttransfection. At 48 h posttransfection, the cell culture medium was collected and mixed with dextran (final concentration 16.25 μg/ml, DEAE-Dextran chloride, molecular weight ~500 kDa; ICN Biomedicals Inc., Aurora, Ohio, USA). The TZM-bl cells were plated in 96-well plates at 500 cells per well in a volume of 100 μl a day before infection. The virus and KD-247 were mixed in a volume of 50 μl and incubated at 37°C for 30 min. Then, the TZM-bl cells were exposed to the virus-KD-247 mixture. At 3 days postinfection, luciferase activity was measured using the Steady-Glo Luciferase Assay system (Promega, Madison, Wisconsin, USA). The IC_{50} was defined as the Nab concentration that yielded a half-reduction in luciferase activity compared with the control wells after subtracting background signals as previously described [12]. Luminescence was detected using a Veritas Microplate Luminometer (Promega). The GHOST cell-based and peripheral blood mononuclear cell-based neutralization assays were performed as described previously [3].

Virus capture ELISA

The ELISA plate (Nunclon, Roskilde, Denmark) was coated by KD-247 with incubating plates with 100 μl of KD-247 preparation (10 μg/ml) in a carbonate buffer (15 mmol/l Na_2CO_3, 35 mmol/l $NaHCO_3$, pH 9.6) at 4°C overnight. Plates were washed five times with Plate Wash Buffer (Zeptometrics, Buffalo, New York, USA), and blocked with PBS containing 20% FBS (Nalgene, Rochester, New York) at 37°C for 1 h. After washing the plates for five times with Plate Wash Buffer and once with PBS, virus was captured by KD-247 by incubating plates with viral preparations containing 50 ng of $p24^{CA}$ resuspended in a volume of 100 μl PBS. After washing PBS with 10% FBS, captured virus was lysed in a buffer and a $p24^{CA}$ ELISA was conducted according to the manufacturer's protocol (Zeptometrics).

Results

Construction of a functional Env library based on the AD8 strain

In theory, it is possible to identify NNR mutations conferring viral resistance to the Nab by selecting Nab-resistant mutants from a Nab-sensitive virus in culture. However, this approach is not ideal for the identification of many NNR mutations at the same time because it primarily selects epitope mutants and only a few dominant NNR mutants. To overcome this problem, we tried to identify NNR mutations that sensitize HIV-1 to KD-247. To achieve this goal, we generated a functional Env library and tried to identify KD-247-sensitizing NNR mutations by correlating mutations with viral susceptibility to KD-247-mediated neutralization. We chose a KD-247-resistant strain, AD8, that shows sequence-neutralization susceptibility discordance, and its IC_{50} to KD-247, when the virus is produced in 293T cells from a proviral DNA, was 354.9 μg/ml by TZM-bl assay (average of five independent experiments). Interestingly, this strain has been reported to be sensitive to 447–52D, which targets the same neutralization epitope within the V3 loop [10]. This suggests that the GPGR epitope of the V3 loop is open to antibodies, and the hindrance of KD-247 epitope is unlikely.

An Env mutant library can be produced by genetic engineering (e.g., PCR-based random mutagenesis). However, such an approach does not always produce functional Env. In contrast, Env mutants generated by viral diversification in tissue culture should be functional unless sporadic mutations that interfere with Env function are introduced. We took the latter approach to generate a functional Env library. We diversified AD8 viruses by approximately 100 passages in MOLT-4 cells. This was a simple bulk passage of virus, whereby tissue culture supernatant was transferred to fresh cells, likely conferring the survival of random mutations. We examined the diversity by sequencing 56 *env* clones. Of these 56 clones, 54 *env* clones were independent, suggesting that the diversification of *env* was successful. The IC_{50} of diversified AD8 to KD-247 was 334.6 μg/ml by TZM-bl assay (average of three independent experiments), suggesting that the diversified AD8 is resistant to KD-247 when scored in bulk. Our data indicate that long-term viral selection in tissue culture does not necessarily select a few dominant mutants; various mutants of independent origins can be maintained. We expected that most of the amino acid substitution mutations should not damage Env function; otherwise, they should not have been selected in culture. The average number of mutations was 3.0 per clone, including the frameshift and stop codon mutations, and, importantly, every virus retained the GPGR epitope in the V3 loop. These viruses were distinct from each other but not as divergent as a panel of field isolates, making them suitable for the identification of KD-247-sensitizing NNR mutations. Our diversification protocol does not necessarily select Env mutants with higher or lower susceptibility to KD-247. We expect that some (but not all) mutations may increase the susceptibility to KD-247. We next evaluated whether any mutations could confer the increased susceptibility of the AD8 strain to KD-247.

Identification of nonepitope neutralization regulatory mutations in various domains of gp120

In our viral diversification protocol, mutations can occur in any region of the viral genome. We are concerned that non-Env mutations could affect neutralization susceptibility to KD-247. For example, the IC_{50} could be scored lower if the viral fitness is poor and higher if viral fitness is high. To avoid these possibilities, we cloned diversified Env into the same viral genetic background. We chose HIV-1_{NL4-3} because it is one of the standard molecular clones of HIV-1, and the proviral DNA is relatively stable and, thus, suitable for such cloning. The AD8 *env* cloned HIV-1_{NL4-3} was named NL/AD8. At first, we verified that the susceptibility of viral isolates to KD-247-mediated neutralization could be reproduced on the HIV-1_{NL4-3} genetic background. For this purpose, we used HIV-1_{MN} and AD8 Env, which are highly susceptible and resistant to KD-247, respectively. Cloning *env* from KD-247-sensitive HIV-1_{MN} into HIV-1_{NL4-3} reproduced neutralization susceptibility (IC_{50} 0.07 μg/ml). Similarly, the KD-247 resistance seen in the AD8 strain was reproduced in the NL/AD8 viruses (IC_{50} 357.5 μg/ml, Table 1). Env mutants with no stop codon or frameshift were tested on the HIV-1_{NL4-3} background. Chimeric viruses carrying AD8 Env mutants that did not yield and infectivity index in TZM-bl cells comparable to that of viruses carrying NL4–3/AD8 were not tested further. Viruses bearing combinations of mutations were generated by positioning mutations between useful restriction enzyme recognition sites in the viral genome. Finally, we examined 27 molecular clones by substituting HIV-1_{NL4-3} *env* with the diversified AD8 *env* clones or AD8 *env* with a point mutation found in the diversified pool (Table 1) Mutations causing Env amino acid changes did not comutate the viral proteins encoded in the Env-overlapping frames including *vpu, tat,* and *rev.*

We determined the IC_{50} of KD-247 on these viruses using TZM-bl cells. Out of 27 viruses, 19 increased their susceptibility to KD-247-mediated neutralization to more than two-fold that of NL/AD8 (19 of 27 clones, 70.4%; Table 1), consistent with previous reports suggesting that the long-term passages *in vitro* select Nab-susceptible HIV-1 [13,14]. Comparing the IC_{50} for each of the mutations, we identified nine NNR mutations that sensitized viruses to KD-247 by more than two-fold (nine of 30 mutations, 30.0%; Table 2). A mutation that altered the IC_{50} no more than two-fold was defined as a non-NNR mutation. Seventeen

Table 1. Summary of half-inhibitory concentration of mutant viruses against KD-247 and b12.

	KD-247		b-12	
Mutations[a]	IC_{50} (μg/m)[b]	Fold sensitization[c]	IC_{50} (μg/m)[b]	Fold sensitization[c]
NL/AD8	357.5 ± 121.8	1	2.4 ± 1.0	1
T48A, D163N, R248M, N297S, S370N, A721T	0.03 ± 0.02	12 342.2	0.2 ± 0.1	12.6
T48A, S186R, S302G S370N, F764S*	7.0 ± 5.5	50.8	0.7 ± 0.2	3.3
S370N, K428E, Q504R, A509T, G689S	39.8 ± 25.9	9.0	1.0 ± 0.3	2.3
D163G, R300G, S370N, S760G	4.4 ± 3.9	82.1	0.4 ± 0.1	6.0
K285R, N298Y, I488T, E506K	480.9 ± 27.1	0.7	1.8 ± 1.1	1.3
E31G, T48A, N279T	141.4 ± 53.1	2.5	1.0 ± 0.2	2.5
D181G, N298Y, S760G	350.0 ± 173.2	1.0	1.8 ± 0.9	1.3
S186R, S370N, S760G	102.8 ± 8.1	3.5	NT	
N298Y, S370N, S760G	380.9 ± 70.7	0.9	1.9 ± 1.0	1.3
V178A, N298Y	89.0 ± 29.3	4.0	8.7 ± 0.9	0.3
N191D, N298Y	157.2 ± 76.8	2.3	1.5 ± 0.9	1.6
I280M, S370N	284.6 ± 34.3	1.3	6.4 ± 0.5	0.4
N297S, S370N	2.4 ± 1.8	149.0	0.8 ± 0.2	3.0
N298Y, E655G*	428.1 ± 47.5	0.8	1.1 ± 0.0	2.3
S370N, N391S	280.5 ± 29.6	1.3	2.5 ± 1.9	1.0
S370N, I546V	303.6 ± 60.8	1.2	2.0 ± 0.2	1.2
S370N, A580T	81.3 ± 18.0	4.4	2.6 ± 0.7	0.9
D163G	6.0 ± 3.5	59.4	1.3 ± 0.0	1.9
D163N	4.8 ± 2.4	74.3	0.9 ± 0.4	2.6
S186R	46.7 ± 24.4	7.7	1.0 ± 0.3	2.4
R248M	59.7 ± 35.8	6.0	2.6 ± 0.7	0.9
N297S	3.0 ± 1.4	119.2	1.2 ± 0.5	2.1
R300G	68.8 ± 28.1	5.2	2.2 ± 1.2	1.1
S302G	6.6 ± 3.4	54.4	2.2 ± 1.1	1.1
S370N	211.5 ± 92.1	1.7	1.2 ± 0.5	2.0
K428E	39.3 ± 35.0	9.1	2.1 ± 0.1	1.2
Q504R	121.6 ± 38.5	2.9	2.7 ± 1.0	0.9

IC_{50}, half-inhibitory concentration; NT, not tested.
[a]NL/AD8 was used as a reference. The amino acid numbering is according to HIV-1AD8 Env. The virus without an asterisk was subjected to virus–antibody binding experiment shown in Fig. 1.
[b]The average and SD from two to 13 independent experiments are shown.
[c]The IC_{50} of the control virus was divided by IC_{50} of each mutant.

Table 2. Summary of mutations characterized in this study.

Mutations[b]	HXB2 coordinate	Location in Env[a]	Fold sensitization
NNR			
D163G	G167	V1/V2	59.4
D163N	G167	V1/V2	74.3
S186R	K192	V1/V2	7.7
R248N	R252	C2	7.0
N297S	N301	V3	119.2
R300G	R304	V3	5.2
S302G	R306	V3	54.4
K428E	K432	C4	9.1
Q504R	Q507	C5	2.9
Non-NNR			
E31G[c]	E32	C1	–
T48A[c]	T49	C1	–
V178A[c]	I181	V1/V2	–
D181G	D185	V1/V2	–
N191D[c]	S195	V1/V2	–
K285R	N289	V3	–
N298Y	N302	V3	–
S370N	S375	C3	–
N391S	X396	V4	–
I488T	I491	C5	–
E506K	E509	C5	–
A509T[c]	A512	gp41	–
I546V	I548	gp41	–
A580T[c]	A582	gp41	–
E655G	E657	gp41	–
G689S[c]	G691	gp41	–
S760G	S762	gp41	–

NNR, nonepitope neutralization regulatory.
[a]The gp120 was subdivided into C1, V1/V2, C3, V3, C4, V4, and C5.
[b]NNR mutations conferring a change in neutralization susceptibility of more than two-fold. Non-NNR mutations are defined as mutations conferring a change in neutralization susceptibility of no more than two-fold.
[c]Estimated from the fold sensitization of a mutant carrying multiple mutations.

non-NNR mutations were also found (Table 2). The magnitude of sensitization by NNR mutations ranged from 2.9 to 119.2. These NNR mutations were present in a broad range of gp120 sites, including V1/V2 loop, C2, V3 loop, C4, and C5. When combined, the NNR mutations additively sensitized the virus to KD-247 by up to 10 000-fold, suggesting an independent structural cross-talk between the V3 loop and each NNR mutation. Such a drastic effect was not observed against b12 Nab targeting the CD4-binding site of gp120 (Table 1). The effect of these NNR mutations appeared to be specific to KD-247, as evidenced by the statistically insignificant correlation between IC_{50} values for KD-247 and b12 (Supplementary Information S1, http://links.lww.com/QAD/A180). This is probably due to the conserved nature of the b12 epitope structure and function. It should be noted that infection with mutant viruses yielded similar levels of luciferase signal from TZM-bl cells when comparable amounts of viruses were used. Also, the viruses bearing six mutations (T48A, D163N, R248M, N297S, S370N, and A721T) replicated in MOLT-4/CCR5 cells with similar efficiency to the no mutation control (NL/AD8), suggesting that replication competency can not account for the change in neutralization susceptibility (data not shown).

Correlation between neutralization susceptibility and KD-247 binding affinity to the virion

We investigated how NNR mutations could sensitize a virus to KD-247-mediated neutralization. We tested whether the KD-247-sensitizing NNR mutation could induce a conformational change in gp120 in such a way that KD-247 became able to bind to gp120 with higher efficiency. To address this question, we performed a capture ELISA in which ELISA plates were precoated with KD-247 and blocked, followed by incubation of virions bearing NNR mutations in the wells of the ELISA plate. The amount of KD-247 captured virus was quantified by ELISA detecting the viral core antigen (Fig. 1). If the latter model is correct, KD-247 captures every mutant with similar efficiencies. As a result, viral binding to KD-247 was significantly correlated with neutralization susceptibility ($P < 0.01$, $n = 26$, two-tailed Student's *t*-test; Fig. 1). These data support a model in which KD-247-sensitizing NNR mutations alter the steady-state structure of gp120 into a conformation such that KD-247 is able to bind to its target with higher efficiencies.

Structural analysis of nonepitope neutralization regulatory mutations

To gain insight into the potential mechanisms whereby KD-247-sensitizing mutations enable neutralization of virions, we used the three-dimensional structural model described by Blay *et al.* [15]. We used an X-ray crystallographic structure with variable loops [15], which was aligned in a trimeric form in accordance with a model developed by Pancera *et al.* [16].

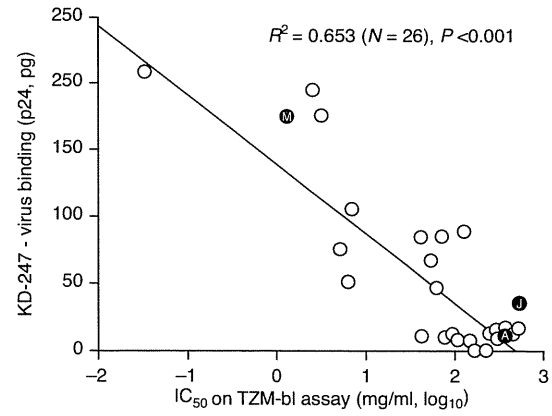

Fig. 1. Analysis of neutralization susceptibility of HIV-1 to KD-247. The half-inhibitory concentration (IC_{50}) for each virus for KD-247 is plotted against the virus capture ELISA data using KD-247 as summarized in Table 1. A significant correlation between the two parameters was detected ($P < 0.01$, two-tailed Student's *t*-test). HIV-1_{MN}, HIV-1_{JR-FL}, and HIV-$1_{NL/AD8}$ are shown as M, J, and A, respectively.

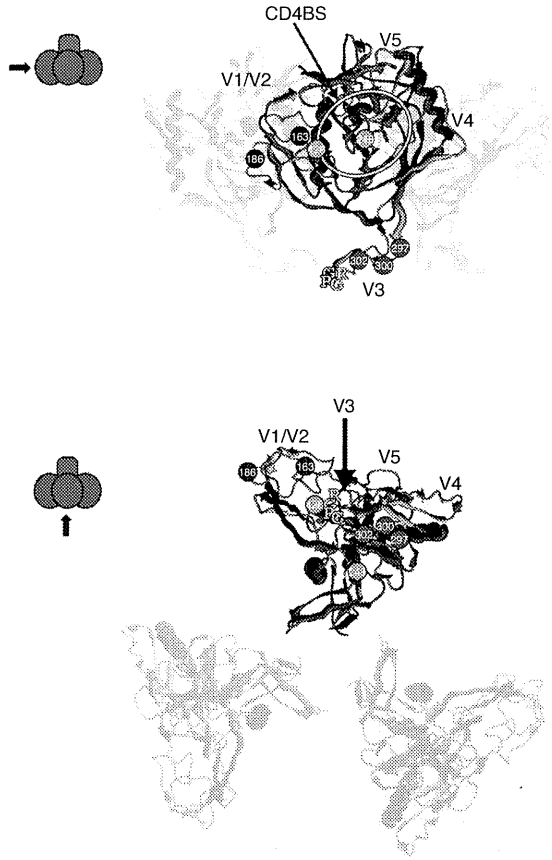

Fig. 2. The three-dimensional mapping of KD-247-sensitizing non-epitope neutralization regulatory mutations based on the Env structure aligned in a trimeric form. The view angle is indicated on the left (arrows) where the gp120 and gp41 are shown in sphere (purple) and rectangle (red), respectively. The gp120 core was shown in blue and red, and the variable loops are shown in yellow. KD-247-sensitizing non-epitope neutralization regulatory (NNR) mutations are indicated by their amino acid numbers. The NNR mutations on the V1/V2 loop, V3 loop, and gp120 core are shown in blue, red, and green, respectively. The GPGR on the V3 loop is shown as a letter code in yellow. The approximate CD4-binding site (CD4BS) is indicated by a white line. The original structural image was developed by Blay *et al.* [15]

The R248N in the C2 region is placed on the gp41 side of the gp120 surface and is not facing the trimeric interface of gp120 (Fig. 2, green) [15]. It has been reported that the H66N, positioned near the trimeric interface of gp120, induces a conformational change of gp120 [17,18]. It has been proposed that H66N alters the quaternary Env structure by acting intermolecularly rather than intramolecularly. In contrast to H66N, the R248N is not positioned at or close to the trimeric surface of gp120. It is likely that R248N induces a different conformational change of the gp120 from H66N, one that does not affect the neutralization susceptibility to b12. It is of interest that the remote KD-247-sensitizing NNR mutation of the gp120 core can specifically affect the conformation of the V3 loop positioned on the gp120 surface.

K428E in the C4 region was mapped in the CD4-binding site close to the so-called bridging sheet (Fig. 2, green), suggesting that the V3 loop and CD4-binding site neutralization epitopes can influence each other's conformation under steady-state conditions. Like R248N, K428E is not positioned at or close to the gp120 trimeric interface. Thus, we speculate that K428E induces a local, not global, Env conformational change. The amino acid corresponding to K428 has been implicated previously in b12 binding through its side-chain as well as through CD4, using HXBc2 Env as a model [19,20]. K428E induces a drastic change in side-chain properties. However, K428E did not significantly affect the viral susceptibility to b12 and the replication efficiency of the NL/AD8 backbone, suggesting that this amino acid may not play a significant role in AD8 Env–b12 interaction. K428 is positioned at the edge of the b12–Env or CD4–Env contact region and, thus, may not contribute significantly to b12–Env or CD4–Env interaction in the context of AD8 Env. Structural cross-talk between the V3 loop and the C4 region under steady-state conditions has been suggested by two studies using monoclonal antibodies. Our approach pinpointed the amino acids responsible for this inter-domain cross-talk.

In contrast to the above two mutations, the precise positioning of KD-247-sensitizing NNR mutations in the V1/V2 and V3 loop is unclear because structural information for them are lacking in the original crystallographic data. According to the molecular dynamics modeling [15], the KD-247-sensitizing NNR mutations in the V1/V2 and V3 loop may not be positioned at or close to the trimeric surface of gp120 (Fig. 2). Instead, they function intramolecularly to affect the conformation of the KD-247 epitope. The Q504R is also lacking in the X-ray crystal structures. However, Q504R is next to the gp120/41 cleavage site and should be close to gp41. The gp41 is relatively proximal to the CD4-binding site of gp120. Some of the mutations in gp41, including T569A and I675V, have been reported to influence the viral susceptibility to Nabs, including b12 [21]. It is conceivable that these mutations in gp41 affect the conformation of gp120. In contrast to T569A and I675V, Q504R is not a b12-sensitizing NNR mutation. Therefore, the conformational change of gp120 induced by Q504R should be distinct from the gp41 mutations.

The structural approach has a potential limitation because the molecular model of Env does not represent the native structure but the liganded structure (Fig. 2). In fact, almost all of the deposited X-ray crystallographic structures are devoid of V1/V2 and/or V3 loops and do not represent the native Env structure, including

the model that our figure is built upon [4,8,15,16,19,22–24].

Discussion

In this work, we identified a number of KD-247-sensitizing NNR mutations using a functional Env library. We re-examined KD-247-sensitive or KD-247-resistant GPGR-positive HIV-1 isolates for NNR mutations and found that KD-247-sensitive viruses, MN (a tissue culture adapted strain of MN) and MNp (a primary HIV-1 isolate), had the mutation equivalent to N301S [25,26]. The predictive value for KD-247 susceptibility due to this mutation was high in the clade B population. However, this does not apply to CRF01_AE, suggesting that this mutation is a clade B-specific predictor of viral susceptibility to KD-247. The other KD-247-sensitizing NNR mutations identified in AD8 did not fully account for the neutralization susceptibility of all of the HIV-1 primary isolates. This suggested that additional NNR mutations should be present, and/or NNR mutations in a given individual virus may function differently than in the other viruses.

How do these mutations alter the conformation of Env to increase the susceptibility of virus to KD-247-mediated neutralization? AD8 is originally resistant to KD-247. One of the molecular mechanisms of AD8 resistance to KD-247 is an epitope-masking by other gp120 domains, possibly the V1/V2 loop or polysaccharides attached to the gp120 [6,27]. Recently, however, Gorny *et al.* [28] reported that the V3 loop of AD8 Env is accessible to KD-247, as AD8 is susceptible to 447–52D-mediated neutralization. This clearly suggests that the sensitization of AD8 strain to KD-247 by the NNR mutations we identified is unlikely due to the removal of the Env domains that physically block antibody access to GPGR epitope. We assume that the V3 loop forms a local conformation in which the neutralization epitope of KD-247 is buried or cannot be recognized by a Nab (local epitope conformation model). When the KD-247-sensitizing NNR mutation occurs, it induces a local, not a global, conformational change of the V3 loop that exposes the neutralization epitope of KD-247. Most of the KD-247-sensitizing NNR mutations are remote from V3 loop. Thus, we assume that KD-247-sensitizing NNR mutations may be located at or close to the interdomain contact regions, and regulate the local conformation of the V3 loop indirectly. Although proven by X-ray crystallographic studies, we propose that the steady-state Env structure is regulated such a way that the domain-independent structural fluctuation is limited. This model predicts that the steady-state structure of the V3 loop is relatively rigid and that its local conformational fluctuation is restricted. This model is relevant to understand the mechanism of action of other NNR mutations against array of Nabs [6–11].

Much attention has been paid to the structural dynamics of HIV-1 Env on CD4 and/or Nab binding. In contrast, not as much attention has been paid to the steady-state conformational dynamics of Env. Unlike previous studies, ours focuses on the steady-state conformational regulation of Env. X-ray crystallography is the best approach to solve a high-resolution native Env structure. However, technical hurdles prevent us from doing so for HIV-1 Env. We examined the mechanism by which the Env conformation is regulated by utilizing Nab KD-247 as a probe. Our approach to identify NNR mutations should complement the crystallization approach in achieving a better understanding of the steady-state structure of HIV-1 Env. Revealing the native structure of Env is critical to the design of an immunogen for the AIDS vaccine and to an understanding of how Env supports virus–cell membrane fusion from the receptor-unbound state.

Acknowledgements

The authors would like to thank Dr Nancy Haigwood for kindly providing the Env structural data. M.T., K.M., E.U., S.K., K.K., S.N., and J.K. designed and performed experiments. T.M., M.H., N.Y., and J.K. analyzed data. J.K. wrote the manuscript.

Conflicts of interest

This work was supported in part by the Japan Health Science Foundation, the Japanese Ministry of Health, Labor and Welfare (H18-AIDS-W-003 and H20-AIDS-G-008 to JK), and the Japanese Ministry of Education, Culture, Sports, Science and Technology (18689014 and 18659136 to J.K.).

There are no conflicts of interest.

References

1. Euler Z, Bunnik EM, Burger JA, Boeser-Nunnink BD, Grijsen ML, Prins JM, *et al.* **Activity of broadly neutralizing antibodies, including PG9, PG16 and VRC01, against recently transmitted subtype B HIV-1 variants from early and late in the epidemic.** *J Virol* 2011; **85**:7236–7245.
2. Hartley O, Klasse PJ, Sattentau QJ, Moore JP. **V3: HIV's switch-hitter.** *AIDS Res Hum Retroviruses* 2005; **21**:171–189.
3. Moore PL, Gray ES, Morris L. **Specificity of the autologous neutralizing antibody response.** *Curr Opin HIV AIDS* 2009; **4**:358–363.
4. Moscoso CG, Sun Y, Poon S, Xing L, Kan E, Martin L, *et al.* **Quaternary structures of HIV Env immunogen exhibit conformational vicissitudes and interface diminution elicited by ligand binding.** *Proc Natl Acad Sci U S A* 2011; **108**:6091–6096.
5. Walker LM, Phogat SK, Chan-Hui PY, Wagner D, Phung P, Goss JL, *et al.* **Broad and potent neutralizing antibodies from an African donor reveal a new HIV-1 vaccine target.** *Science* 2009; **326**:285–289.

6. Walker LM, Burton DR. **Rational antibody-based HIV-1 vaccine design: current approaches and future directions.** *Curr Opin Immunol* 2010; **22**:358–366.
7. Willey S, Aasa-Chapman MM. **Humoral immunity to HIV-1: neutralization and antibody effector functions.** *Trends Microbiol* 2008; **16**:596–604.
8. Zhou T, Georgiev I, Wu X, Yang ZY, Dai K, Finzi A, *et al.* **Structural basis for broad and potent neutralization of HIV-1 by antibody VRC01.** *Science* 2010; **329**:811–817.
9. Wei X, Decker JM, Wang S, Hui H, Kappes JC, Wu X, *et al.* **Antibody neutralization and escape by HIV-1.** *Nature* 2003; **422**:307–312.
10. Gorny MK, Revesz K, Williams C, Volsky B, Louder MK, Anyangwe CA, *et al.* **The v3 loop is accessible on the surface of most human immunodeficiency virus type 1 primary isolates and serves as a neutralization epitope.** *J Virol* 2004; **78**:2394–2404.
11. Gray ES, Moore PL, Bibollet-Ruche F, Li H, Decker JM, Meyers T, *et al.* **4E10-resistant variants in a human immunodeficiency virus type 1 subtype C-infected individual with an antimembrane-proximal external region-neutralizing antibody response.** *J Virol* 2008; **82**:2367–2375.
12. Martin L, Stricher F, Misse D, Sironi F, Pugnière M, Barthe P, *et al.* **Rational design of a CD4 mimic that inhibits HIV-1 entry and exposes cryptic neutralization epitopes.** *Nat Biotechnol* 2003; **21**:71–76.
13. Wrin T, Loh TP, Vennari JC, Schuitemaker H, Nunberg JH. **Adaptation to persistent growth in the H9 cell line renders a primary isolate of human immunodeficiency virus type 1 sensitive to neutralization by vaccine sera.** *J Virol* 1995; **69**:39–48.
14. Zhang YJ, Fredriksson R, McKeating JA, Fenyo EM. **Passage of HIV-1 molecular clones into different cell lines confers differential sensitivity to neutralization.** *Virology* 1997; **238**:254–264.
15. Blay WM, Gnanakaran S, Foley B, Doria-Rose NA, Korber BT, Haigwood NL. **Consistent patterns of change during the divergence of human immunodeficiency virus type 1 envelope from that of the inoculated virus in simian/human immunodeficiency virus-infected macaques.** *J Virol* 2006; **80**:999–1014.
16. Pancera M, Majeed S, Ban YE, Chen L, Huang CC, Kong L, *et al.* **Structure of HIV-1 gp120 with gp41-interactive region reveals layered envelope architecture and basis of conformational mobility.** *Proc Natl Acad Sci U S A* 2010; **107**:1166–1171; Epub 2010 Dec 28..
17. Kassa A, Finzi A, Pancera M, Courter JR, Smith AB 3rd, Sodroski J. **Identification of a human immunodeficiency virus type 1 envelope glycoprotein variant resistant to cold inactivation.** *J Virol* 2009; **83**:4476–4488.
18. Kassa A, Madani N, Schon A, Haim H, Finzi A, Xiang SH, *et al.* **Transitions to and from the CD4-bound conformation are modulated by a single-residue change in the human immunodeficiency virus type 1 gp120 inner domain.** *J Virol* 2009; **83**:8364–8378.
19. Zhou T, Xu L, Dey B, Hessell AJ, Van Ryk D, Xiang SH, *et al.* **Structural definition of a conserved neutralization epitope on HIV-1 gp120.** *Nature* 2007; **445**:732–737.
20. Wu X, Zhou T, O'Dell S, Wyatt RT, Kwong PD, Mascola JR. **Mechanism of human immunodeficiency virus type 1 resistance to monoclonal antibody B12 that effectively targets the site of CD4 attachment.** *J Virol* 2009; **83**:10892–10907.
21. Blish CA, Nguyen MA, Overbaugh J. **Enhancing exposure of HIV-1 neutralization epitopes through mutations in gp41.** *PLoS Med* 2008; **5**:e9.
22. Cho YK, Foley BT, Sung H, Kim YB, Kim JH. **Molecular epidemiologic study of a human immunodeficiency virus 1 outbreak in haemophiliacs B infected through clotting factor 9 after 1990.** *Vox Sang* 2007; **92**:113–120.
23. Huang CC, Tang M, Zhang MY, Majeed S, Montabana E, Stanfield RL, *et al.* **Structure of a V3-containing HIV-1 gp120 core.** *Science* 2005; **310**:1025–1028.
24. Diskin R, Marcovecchio PM, Bjorkman PJ. **Structure of a clade C HIV-1 gp120 bound to CD4 and CD4-induced antibody reveals anti-CD4 polyreactivity.** *Nat Struct Mol Biol* 2010; **17**:608–613.
25. Leavitt M, Park EJ, Sidorov IA, Dimitrov DS, Quinnan GV Jr. **Concordant modulation of neutralization resistance and high infectivity of the primary human immunodeficiency virus type 1 MN strain and definition of a potential gp41 binding site in gp120.** *J Virol* 2003; **77**:560–570.
26. Eda Y, Takizawa M, Murakami T, Maeda H, Kimachi K, Yonemura H, *et al.* **Sequential immunization with V3 peptides from primary human immunodeficiency virus type 1 produces cross-neutralizing antibodies against primary isolates with a matching narrow-neutralization sequence motif.** *J Virol* 2006; **80**:5552–5562.
27. Kwong PD, Wyatt R, Robinson J, Sweet RW, Sodroski J, Hendrickson WA. **Structure of an HIV gp120 envelope glycoprotein in complex with the CD4 receptor and a neutralizing human antibody.** *Nature* 1998; **393**:648–659.
28. Gorny MK, Williams C, Volsky B, Revesz K, Cohen S, Polonis VR, *et al.* **Human monoclonal antibodies specific for conformation-sensitive epitopes of V3 neutralize human immunodeficiency virus type 1 primary isolates from various clades.** *J Virol* 2002; **76**:9035–9045.